JOURNAL OF COMPUTATIONAL PHYSICS **129,** 134–159 (1996)
ARTICLE NO. 0239

Higher-Order Exponential Difference Schemes for the Computations of the Steady Convection–Diffusion Equation

Yao-Hsin Hwang

Chung Shun Institute of Science and Technology, Lung Tan 90008-15-1, Taiwan 32526, Republic of China

Received January 24, 1996; revised June 14, 1996

Conventional exponential difference schemes may yield accurate and stable solutions for the one-dimensional, source-free convection–diffusion equation. However, its accuracy will be deteriorated in the presence of a nonconstant source term or in multidimensional problems. Attempts are made to increase the accuracy of exponential difference schemes. First, we propose an exponential difference scheme that retains second-order accuracy in the presence of a source term or in multidimensional situations. Mathematical analysis and numerical experiments are performed to validate this scheme. Second, a local particular solution method is introduced to raise the solution accuracy for problems with a source term. This method locally transforms the original problem to a source-free one, to which an accurate solution can be obtained. Performance of this process is verified by numerical calculations of some test problems. Third, two skew exponential difference schemes are proposed to raise the solution accuracy in multidimensional problems: one is designed to be free of numerical diffusion and the other with minimum numerical diffusion to ensure solution monotonicity. Comparisons with existing schemes are performed by conducting numerical experiments on several test problems. Finally, a simple blending procedure of these two schemes is suggested to yield an accurate and stable representation of the convection–diffusion problem in all possible situations, with or without solution discontinuities.

1. INTRODUCTION

In practical engineering applications, convection–diffusion equations are generally employed to describe the transport processes involving fluid motion. With the progress in computer power, the differential convection–diffusion equations can be analytically studied by pursuing the numerical solutions of their discretized counterparts. Therefore, accurate and stable difference representations of the convection–diffusion equations are of vital importance. By inspecting the convection–diffusion equation, one can find that it contains two distinct differential operators derived from their respective physical processes: the convection and the diffusion operators. The convection operator consists of first-order spatial derivatives of the transported variables, which arise from the fluid flow motion. On the other hand, the diffusion operator is represented by second-order spatial derivatives due to transports at the molecular level. These two terms are treated separately and then combined to form the resulting discretized expression in the conventional finite difference formulation. For the diffusion term, the central difference scheme (CD) can provide an accurate and stable discretized representation. This central difference expression has a compact three-point supported stencil in one dimension and yields second-order accuracy in space. The resulting matrix equation is diagonally dominant and can be solved by simple iterative methods. With this diagonal dominance property, bounded solutions can be easily achieved. Similar central difference formulation can be applied for the convection term and the resulting difference equation can also be proven to be second-order accurate. However, if the flow velocity is quite large or the grid spacing is not suitably refined, nonphysical spurious oscillation can be found in the resulting solution which reflects erroneous processes [1]. This phenomenon is designated as the boundedness problem for the occurrence of an oscillatory solution. Moreover, difficulties in the convergence may occur if the system of equations are solved by an iterative method, such as Gauss–Seidel or alternating direction implicit (ADI), unless heavy relaxation between two successive iterations is applied [2]. This phenomenon can be physically attributed to the symmetrical influence weighting of neighboring points in the central difference scheme for the diffusion term, which obviously violates the unsymmetrical nature of the convection operator. The diagonal dominance in the resulting matrix equations is no longer satisfied since the downstream influence coefficient becomes negative.

To circumvent the problem of an unbounded solution from the central difference representation, some kind of upstream discretized expression should be considered to account for the inherent physical nature of the convection operator. A simple and physically reasonable upwind difference scheme (1UD) is well known [3]. Although this is a robust and unconditionally stable scheme for all flow velocities and grid spacings, its accuracy is found to be only first order. Significant numerical diffusion is introduced and may obscure the physical diffusion in the computational results. A compromise between CD and 1UD for

0021-9991/96 $18.00

the convection term is proposed by Spalding [4] who adopted CD in the situation where the flow velocity is not large or the grid spacing is appropriately refined, and 1UD in case of CD is prone to be unstable. In practical computations, however, the gain in numerical accuracy by this hybrid combination over the 1UD scheme is quite limited. Meanwhile, it is known from numerical experiments [5, 6] that an accurate solution of these upwind schemes is difficult to achieve. Therefore, higher-order accurate upwind schemes free of numerical diffusion will be beneficial to present the convection operator. Leonard [7], therefore, devised a quadratic upstream interpolation for convective kinematics (QUICK) scheme based on a finite-volume formulation. The interface quantities conveyed by the flow motion are interpolated by a quadratic distribution, based on those at two upstream and one downstream computational locations. Atias *et al.* [8] used upstream linear extrapolation to depict the interface quantities and created a second-order accurate upwind difference scheme (2UD). Although the 2UD scheme was criticized by Gupta and Manohar [9] for its numerical accuracy and stability with some simple mathematical analyses, it possesses some interesting features shown by the numerical experiment in Shyy [10]. Higher-order schemes can be derived by incorporating more computational nodes [11–14]; however, these two upwind schemes (QUICK and 2UD) are still widely used by computational fluid dynamic communities to simulate the convection term [15–17]. Besides, there are some additional disadvantages for these high-order schemes. First, these schemes involve more computational points than the CD or 1UD schemes and increase the computational load and programming complexity. Second, since more computational nodes are included in the finite difference stencil, these schemes need some low-order schemes to trigger the computational procedure. This is called the starting problem for high-order schemes. The adopted low-order scheme will inevitably induce additional numerical errors near the boundaries which eventually propagate into the computational domain. Third, these schemes suffer from the boundedness problem if the flow velocity is large and there exist some strong gradients in the solution. This disadvantage is a direct consequence of Godunov's theorem on hyperbolic equations, which states that a linear monotone scheme cannot be higher than first-order accurate [18]. These high-order schemes result in some negative influence coefficients for the neighboring computational points in the coefficient matrix equations. Therefore, the diagonal dominance may not be satisfied and computational difficulty may occur if iterative methods are used to solve the resulting difference equations.

All the aforementioned difference schemes are based on one-dimensional analysis. For multidimensional situations, these schemes are applied in each spatial dimension to derive the resulting discretized equations. The first multidimensional scheme was the skew upwind difference scheme (SKUD) proposed by Raithby [19]. In SKUD, the interface quantities are determined by the upstream flow location, based on the velocity vector direction rather than on the split directions. Such consideration can decrease the numerical diffusion and yields more accurate results. However, the problem with an unbounded solution may also exist for this scheme since there is no definite control for the occurrence of negative influence coefficients. This scheme is also widely adopted to calculate practical complicated flows [20–22].

Besides the separate treatment of convection and diffusion terms, one may consider these two terms simultaneously by incorporating a local exact solution for the differential convection–diffusion equations within the finite computational cells. This approach results in the so-called exponential difference scheme (1ED) since the influence coefficients involve exponential functions [23–25]. This scheme has the noteworthy features that it can be simplified to the CD scheme in the case of low flow velocity or sufficiently refined grid and to the 1UD scheme in the high velocity condition. Upwind convection effects are inherently considered in the exponential functions. From the Taylor-series truncation error analysis (TSTE), the apparent accuracy of the 1ED scheme is only first order. However, a deeper investigation of the TSTE will show this scheme provides the exact solution for the one-dimensional convection–diffusion equation in the absence of a source term. This verification is given in the present work. Therefore, the 1ED scheme will yield the exact distribution for the transported variables of the convection–diffusion process no matter how large the flow velocity or grid spacing. But in the presence of a nonconstant source term and in the multidimensional situations its accuracy will be reduced to first order in the high cell Reynolds number situation as depicted by the TSTE. The numerical diffusion effect may overwhelm the physical diffusion, as in the case of the 1UD scheme [7], which is why this original exponential scheme is not suitable for the accurate prediction of complex flows [26]. The situation of the presence of a nonconstant source term will be frequently encountered in the simulation of a flow process with pressure gradient or in moldelling turbulence behavior. Based on this understanding, we propose a local particular solution method to recover the accuracy possessed by the exponential schemes. Meanwhile, a second-order accurate exponential difference scheme (2ED) has also been derived by taking advantage of the inherent upwind nature of the exponential function. The numerical diffusion is eliminated by this scheme in the multidimensional situations. For the high-order difference schemes, the existence of a source term will not deteriorate the formal numerical accuracy depicted by the TSTE. However, the local particular solution

method can also be applied with any high-order scheme to account for the spatial distribution of the source term.

The exact solution of the convection–diffusion equation in a finite multidimensional computational cell needs the information along the boundaries of finite computational volume. However, values of the dependent variable are only defined at computational nodes. Therefore, distributions based on these discrete nodes must be assumed along the finite control surfaces to derive a corresponding ''approximate exact solution''. Stubley *et al.* [27] adopted piecewise linear and quadratic distributions along the boundaries in their linear influence scheme (LIS) and quadratic influence scheme (QIS), respectively. Chen and Chen [28], on the other hand, assume an exponential combined with a linear distribution to derive the finite analytic method (FA). These formulations have been successfully applied to solve some practical flow problems. However, usage of the assumed boundary distribution will induce some numerical errors. The major disadvantage of these schemes is that the derivation of the approximate solutions is achieved by the separation of variables. A large computational load must be devoted to calculate the infinite series to determine the influence coefficients. In some circumstances, there may be difficulties in obtaining a convergent series summation. Therefore, although these schemes can yield accurate solutions, their applications are not very widespread because they are computationally inefficient. In the present study, we will propose two-dimensional exponential schemes similar to LIS, QIS, or FA, without the introduction of assumed boundary profiles. The cumbersome computations of infinite series can be avoided. We regard these schemes as skew exponential schemes (SKED).

Besides the introductory section mentioned above, the content of present paper is organized as follows. In Section 2, we will present a one-dimensional analysis for the difference schemes based on Taylor-series truncation error analysis and their characteristic roots. A second-order accurate exponential difference scheme is then proposed. Simple asymptotic analysis of the general properties of this scheme is also performed. Section 3 deals with the effects of a nonconstant source term on the accuracy of first-order exponential difference scheme. Decrease in the accuracy is illustrated and a local particular solution method is proposed to overcome this problem. A simple polynomial fitting procedure is also suggested to find the local particular solution for general source terms. In Section 4, a two-dimensional analysis is presented based on the cross-stream spurious numerical diffusion. We derive a general expression for the numerical diffusion of skew difference schemes and propose two skew exponential difference schemes to model the convection–diffusion equation. One is designed to be free of numerical diffusion and the other has with minimum numerical diffusion to ensure solution monotonicity. Corresponding numerical diffusivities of some existing schemes are also calculated. A simple blending procedure of these two proposed exponential difference schemes is suggested to provide a more accurate and stable simulation for all possible situations, with or without solution discontinuities. In Section 5, numerical experiments for several one- and two-dimensional test problems are performed to validate the feasibility of the proposed methods. It is shown, from the computational results, that the exponential difference schemes can be employed to provide accurate discretizations of the convection–diffusion equations. Finally, Section 6 is devoted to some concluding remarks.

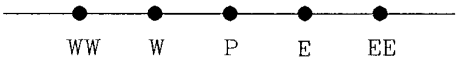

FIG. 1. Computational module for one-dimensional analysis.

2. ONE-DIMENSIONAL ANALYSIS

Consider the steady one-dimensional convection–diffusion equation for a scalar quantity Φ in the absence of source term:

$$L(\Phi) = -R\frac{d\Phi}{dx} + \frac{d^2\Phi}{dx^2} = 0, \tag{1}$$

where R denotes the nondimensional flow velocity which, without loss of generality, is assumed to be positive. The first term is the convection term and the second term is the diffusion term. The present objective is to derive an appropriate discretization for the above equation at the computational point P shown in Fig. 1. The difference formulas considered in the present work can be expressed in the following general form,

$$\begin{aligned} L_h(\phi) = {} & A_{\mathrm{ww}}\phi_{\mathrm{ww}} + A_{\mathrm{w}}\phi_{\mathrm{w}} + A_{\mathrm{E}}\phi_{\mathrm{E}} \\ & + A_{\mathrm{EE}}\phi_{\mathrm{EE}} - A_{\mathrm{P}}\phi_{\mathrm{P}} = 0, \end{aligned} \tag{2}$$

where ϕ is the approximate value of Φ and the A's are the influence coefficients. By Taylor-series expansion at point P, the truncation error for the discretized expression (2) can be written as

$$\begin{aligned} T_h(\Phi_h) = {} & \{[(A_{\mathrm{E}} - A_{\mathrm{W}}) + 2(A_{\mathrm{EE}} - A_{\mathrm{WW}})]h + R\}\frac{d\Phi}{dx} \\ & + \left\{[(A_{\mathrm{E}} + A_{\mathrm{W}}) + 4(A_{\mathrm{EE}} + A_{\mathrm{WW}})]\frac{h^2}{2} - 1\right\}\frac{d^2\Phi}{dx^2} \\ & + \left\{[(A_{\mathrm{E}} - A_{\mathrm{W}}) + 8(A_{\mathrm{EE}} - A_{\mathrm{WW}})]\frac{h^3}{6}\right\}\frac{d^3\Phi}{dx^3} + \mathrm{HOT}, \end{aligned} \tag{3}$$

where Φ_h is the exact solution at the computational points, h is the uniform grid spacing, and HOT denotes the highest-order terms. In this equation, the general relation between the influence coefficients,

$$A_P = A_{WW} + A_W + A_E + A_{WW}, \tag{4}$$

was imposed. Satisfaction of this equation implies the resulting difference equation is independent of the reference value assigned at the boundary. Therefore, for any difference scheme, we can determine its associated truncation error from the influence coefficients. The first term at the RHS of Eq. (3) involving $d\Phi/dx$ can be physically interpreted as the spurious velocity because it is arising from the convection term. The second term, on the other hand, from the diffusion term can then be regarded as the numerical diffusion. Therefore, we may say that a difference scheme is without spurious velocity or numerical diffusion if the first term or the second term in Eq. (3) vanish, respectively.

2.1. *Solution of Discretized Equation*

The exact solution of the discretized equation (2) can be obtained with the generalized form [9, 10]

$$\phi_i = \sum_{n=1}^{M} \alpha_n r_n^i, \tag{5}$$

where i is location index, r_n is the nth characteristic root, α_n is the nth coefficient constant depending on the difference boundary condition, and M is the total number of neighboring points included in the finite difference equation (2). If there exist some characteristic roots with negative sign, the discretized solution may show persistent spurious oscillation between successive even–odd computational locations. Therefore, when any one of the nontrivial characteristic roots becomes zero at a particular cell Reynolds number, this cell Reynolds number can be regarded as the critical cell Reynolds number for this discretized scheme. Substituting the characteristic equation (5) into the finite difference equation (2), we can solve for the characteristic roots after some algebraic manipulations.

A simple interpretation can be devised for the above equations and a general requirement on the influence coefficients for the nonpersistent oscillatory solution can be found. If all the characteristic roots are positive, we can find the following simple relation for the influence coefficients:

$$A_W A_E \geq 0; \quad A_{WW} A_W \leq 0.$$

Since A_W is the nearest upstream influence coefficient, a reasonable difference scheme must satisfy:

$$A_W \geq \mathrm{Max}(|A_{EE}|, |A_E|, |A_{WW}|);$$

that is, A_W should be positive and its magnitude should be the largest of all influence coefficients. Therefore, the general rule for the influence coefficients which allows only positive characteristic roots will be:

$$A_{WW} \leq 0; \quad A_W \geq 0; \quad A_P \geq 0; \quad A_E \geq 0; \quad A_{EE} \leq 0. \tag{6}$$

With this simple rule, the critical cell Reynolds number can be obtained by simply assigning $A_E = 0$, under which condition one of the characteristic roots will change its sign [10].

Generally speaking, the requirement for a nonpersistent oscillatory solution, Eq. (6), is not consistent with that for a monotonic difference scheme, which states that all influence coefficients should be positive. Therefore, a multipoint monotonic scheme may possess negative characteristic roots and show persistent spurious oscillation if the difference boundary condition is not appropriately assigned. However, the oscillatory amplitude in a monotonic difference scheme is constrained by the boundary values. On the other hand, a difference scheme with all positive characteristic roots does not guarantee a bounded solution. The coefficients, α_n in Eq. (5), may have different signs and subsequently induce local extrema. However, the number of local extrema cannot be more than that of the neighboring points involved in the difference equation. That is, the spurious oscillation cannot pollute all the computational domain.

2.2. *The First-Order Exponential Scheme* (1*ED*)

The exponential scheme is derived, based on the exact solution of the steady one-dimensional convection–diffusion equation (1) within the computational cell W-P-E in Fig. 1,

$$\phi(x) = \phi_1(x) + \phi_2(x)$$

with

$$\phi_1(h) = 0, \quad \phi_1(-h) = 1, \tag{7}$$

and

$$\phi_2(h) = 1, \quad \phi_2(-h) = 0,$$

where both $\phi_1(x)$ and $\phi_2(x)$ satisfy the original differential equation (1). This is the superposition technique for solving linear differential equations. The influence coefficient A_W is then proportional to $\phi_1(0)$ and A_E is proportional to $\phi_2(0)$. After solving Eq. (7), we can obtain the general expressions for A_W and A_E,

$$A_W = \alpha \exp\left(\frac{Rh}{2}\right), \quad A_E = \alpha \exp\left(-\frac{Rh}{2}\right), \tag{8}$$

where α is the proportional constant and exp( ) denotes the exponential function. With these simple exponential functions, the upwind nature for the convection effect has been automatically included in Eq. (8), because $A_W > A_E$ if $Rh > 0$. The proportional constant α can be determined by the fact that the resulting discretized equation (2) should approximate the differential equation (3) without inducing spurious velocity, that is,

$$(A_E - A_W)h + R = 0.$$

Therefore, the final influence coefficients for the 1ED scheme are

$$A_{WW} = 0, \quad A_W = \frac{R \exp(Rh/2)}{2h \sinh(Rh/2)}, \quad A_P = \frac{R}{h}\coth\left(\frac{Rh}{2}\right),$$
$$A_E = \frac{R \exp\left(-\frac{Rh}{2}\right)}{2h \sinh(Rh/2)}, \quad A_{EE} = 0; \tag{9}$$

and the truncation error is

$$T_{h,1ED} = \left[\frac{Rh}{2}\coth\left(\frac{Rh}{2}\right) - 1\right]\frac{d^2\Phi}{dx^2} - \frac{Rh^2}{6}\frac{d^3\Phi}{dx^3} + \text{HOT}. \tag{10}$$

The numerical diffusivity for the 1ED scheme is $(Rh/2)\coth(Rh/2) - 1$, which cannot be neglected at high cell Reynolds number, and the effective cell Reynolds number is $2\tanh(Rh/2)$. From the influence coefficients given in Eq. (9), the 1ED scheme will approach the CD scheme at small cell Reynolds number and behaves like a second-order scheme. For high cell Reynolds number, however, the 1ED scheme will approach the 1UD scheme which is only first-order accurate. However, if we consider the exact solution of the one-dimensional convection–diffusion equation without the source term, we have the following relation:

$$\frac{d^n\Phi}{dx^n} = R^{n-1}\frac{d\Phi}{dx}. \tag{11}$$

Substituting this relation into the TSTE in Eq. (10) and collecting the coefficients, we can derive the actual truncation error for the 1ED scheme:

$$T_{h,1ED} = 0. \tag{12}$$

This simple derivation explains why the 1ED scheme can provide the exact solution regardless of the flow velocity and grid spacing. But in practical situations, both the source term and multidimensionality must be considered. The relation given in Eq. (11) is not satisfied generally and the accuracy of the 1ED scheme will reduce to that as depicted by the TSTE analysis. Effects of source term on the accuracy of exponential schemes will be investigated in the present study. In a later section, we will reconsider this problem and propose a simple numerical modification to treat the source term and recover the accuracy of the difference equation.

The characteristic roots for 1ED can be obtained by substituting Eqs. (5) and (9) into Eq. (2):

$$r = 1 \quad \text{or} \quad r = \exp(Rh). \tag{13}$$

Therefore, the 1ED scheme is a monotonic scheme without any negative characteristic root.

2.3. *The Second-Order Exponential Scheme* (2*ED*)

From the derivation of the exponential scheme given above, we find the relative importance of the influence coefficients for the upstream (A_W) and downstream (A_E) computational points in the difference equation. The apparent accuracy can be raised by incorporating more computational points (A_{WW}) and (A_{EE}) in the finite difference equation. The relation of the influence coefficients can be taken as

$$A_W = \alpha_1 \exp\left(\frac{Rh}{2}\right), \quad A_E = \alpha_1 \exp\left(-\frac{Rh}{2}\right),$$
$$A_{WW} = \alpha_2 \exp(Rh); \quad A_{EE} = \alpha_2 \exp(-Rh). \tag{14}$$

The proportional constants, α_1 and α_2, can be determined from the TSTE analysis to satisfy a second-order accurate approximation:

$$A_E - A_W + 2(A_{EE} - A_{WW}) = -R/h,$$
$$A_E + A_W + 4(A_{EE} + A_{WW}) = 2/h^2. \tag{15}$$

The resulting influence coefficients are:

$$A_{WW} = \frac{\frac{1}{h^2}\sinh\left(\frac{Rh}{2}\right) - \frac{R}{2h}\cosh\left(\frac{Rh}{2}\right)}{4\cosh(Rh)\sinh\left(\frac{Rh}{2}\right) - 2\sinh(Rh)\cosh\left(\frac{Rh}{2}\right)}\exp(Rh),$$

A_W

$$= \frac{2\frac{R}{h}\cosh(Rh) - \frac{2}{h^2}\sinh(Rh)}{4\cosh(Rh)\sinh\left(\frac{Rh}{2}\right) - 2\sinh(Rh)\cosh\left(\frac{Rh}{2}\right)} \exp\left(\frac{Rh}{2}\right),$$

A_P

$$= \frac{\frac{1}{h^2}\sinh\left(\frac{Rh}{2}\right) - \frac{R}{2h}\cosh\left(\frac{Rh}{2}\right)}{2\cosh(Rh)\sinh\left(\frac{Rh}{2}\right) - \sinh(Rh)\cosh\left(\frac{Rh}{2}\right)} \cosh(Rh)$$

$$+ \frac{2\frac{R}{h}\cosh(Rh) - \frac{2}{h^2}\sinh(Rh)}{2\cosh(Rh)\sinh\left(\frac{Rh}{2}\right) - \sinh(Rh)\cosh\left(\frac{Rh}{2}\right)} \cosh\left(\frac{Rh}{2}\right),$$

A_E

$$= \frac{2\frac{R}{h}\cosh(Rh) - \frac{2}{h^2}\sinh(Rh)}{4\cosh(Rh)\sinh\left(\frac{Rh}{2}\right) - 2\sinh(Rh)\cosh\left(\frac{Rh}{2}\right)} \exp\left(-\frac{Rh}{2}\right),$$

A_{EE}

$$= \frac{\frac{1}{h^2}\sinh\left(\frac{Rh}{2}\right) - \frac{R}{2h}\cosh\left(\frac{Rh}{2}\right)}{4\cosh(Rh)\sinh\left(\frac{Rh}{2}\right) - 2\sinh(Rh)\cosh\left(\frac{Rh}{2}\right)} \exp(-Rh) \tag{16}$$

with the following truncation error:

$T_{h,2ED}$

$$= -\left[\frac{R}{h} + 6\frac{\frac{1}{h^2}\sinh\left(\frac{Rh}{2}\right) - \frac{R}{2h}\cosh\left(\frac{Rh}{2}\right)}{2\cosh(Rh)\sinh\left(\frac{Rh}{2}\right) - \sinh(Rh)\cosh\left(\frac{Rh}{2}\right)} \sinh(Rh)\right] \frac{h^3}{6}\frac{d^3\Phi}{dx^3} + \text{HOT}. \tag{17}$$

The asymptotic properties of the 2ED scheme developed herein can be analyzed as the cell Reynolds number approaches zero or infinity. As the cell Reynolds number approaches zero, the influence coefficients in Eq. (16) for the 2ED scheme can be simplified to yield the following discretized equation:

$$-\phi_{WW} + 16\phi_W - 30\phi_P + 16\phi_E - \phi_{EE} = 0. \tag{18}$$

This is a fourth-order difference scheme for the pure diffusion problem [12] and its characteristic roots are

$$r = 1, 1, 7 + \sqrt{48}, \text{ and } 7 - \sqrt{48} \tag{19}$$

which are all positive. Therefore, the 2ED scheme can provide a highly accurate and nonoscillatory expression for the diffusion dominated problem. In the limit of pure convection problem ($Rh \to \infty$), the difference equation can be simplified as:

$$-\tfrac{1}{3}\phi_{WW} + \tfrac{4}{3}\phi_W - \phi_P = 0. \tag{20}$$

This expression is identical with the 2UD scheme for $Rh \to \infty$ [8]. This coincidence can be interpreted by observing the influence coefficients given in Eq. (16). The exponential functions imply vanishing of the downstream influence coefficients for large cell Reynolds number. The characteristic roots for this condition are

$$r = 1 \quad \text{or} \quad r = \tfrac{1}{3} \tag{21}$$

which are all positive and indicate that the persistent spurious oscillation will not exist in the difference solution. Therefore, in both limiting cases of pure diffusion and convection problems, the 2ED scheme will be superior to the 2UD scheme, albeit there is higher computational complexity involved for evaluating the exponential functions. These calculations can, nevertheless, be approximated with some simple polynomials as in the case of the power-law scheme approximation for the 1ED scheme [29].

For any value of the cell Reynolds number, the characteristic equation for the 2ED scheme is

$$A_{EE}r^4 + A_E r^3 - A_P r^2 + A_W r + A_{WW} = 0 \tag{22}$$

with the influence coefficients given in Eq. (16). The characteristic roots for this equation can be determined [30] and, except for the constant reference mode $r = 1$, are

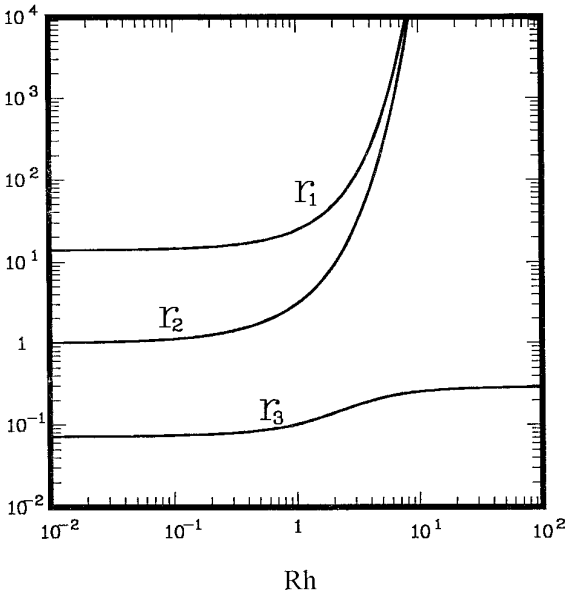

FIG. 2. Characteristic roots for the 2ED scheme.

plotted in Fig. 2 as a function of cell Reynolds number. As shown in Fig. 2, two characteristic roots, r_1 and r_2, will approach infinity with large cell Reynolds number which indicates the singular behavior of Eq. (22) when the downstream coefficients A_E and A_{EE} vanish. The characteristic roots shown in Fig. 2 are all positive, indicating that there is no persistent spurious oscillation in the solution by the 2ED scheme.

Normalized influence coefficients for the one-dimensional schemes considered in the present study (CD, 1UD, 1ED, QUICK, 2UD, and 2ED) are given in Fig. 3. Those for other well-known schemes, CD, 1UD, QUICK, and 2UD can be found from the existing literature [7, 8, 10]. These coefficients have been normalized by their respective diagonal terms such that

$$A_{WW} = \frac{A_{WW}}{A_P}, \quad A_W = \frac{A_{WW}}{A_P}, \quad A_e = \frac{A_E}{A_P}, A_{ee} = \frac{A_{EE}}{A_P}.$$

It can be found from Figs. 3b and 3c that the 1ED scheme will approach the 1UD scheme and, from Figs. 3e and 3f, the 2ED scheme will approach the 2UD scheme as the cell Reynolds number increases. All schemes, except 2ED, will have 3-point stencils as the flow velocity vanishes. For the 2ED scheme, the 5-point stencil remains, giving a highly accurate expression for the diffusion dominated situation. Also note that the nearest downstream influence coefficients, A_E, for the CD and QUICK schemes becomes negative as the cell Reynolds number exceeds their respective critical value ($RH_{c,CD} = 2.$ and $Rh_{c,QUICK} = \frac{8}{3}$) [10].

3. EFFECTS OF SOURCE TERM

One of the major criticisms on the 1ED scheme is that its accuracy will decrease drastically if there exists a strong nonconstant source term in the differential equation [7, 23],

$$L^s(\Phi) = -R\frac{d\Phi}{dx} + \frac{d^2\Phi}{dx^2} + S = 0. \tag{23}$$

Mathematically, with this nonconstant source term, S, the functional relation given in Eq. (11) is no longer satisfied and the accuracy will decrease to that depicted in Eq. (10). In the present study, we propose a natural local particular solution method to recover the accuracy with the 1ED scheme. Consider the differential equation in a finite computational cell as shown in Fig. 1. If a local particular solution ϕ^* can be found satisfying Eq. (23) without any constraint on the boundary condition;

$$L^s(\phi^*) = -R\frac{d\phi^*}{dx} + \frac{d^2\phi^*}{dx^2} + S = 0 \tag{24}$$

then a difference quantity defined as

$$\hat{\phi} = \phi - \phi^* \tag{25}$$

will satisfy the source-free differential equation (1). The 1ED scheme applied to approximate the source-free equation (1) will be identical with the original scheme and show no truncation error,

$$L_h(\hat{\phi}) = 0. \tag{26}$$

Finally, substituting the original variable into the transformed difference equation leads to the difference equation

$$\begin{aligned} L_h^s(\phi) = {} & A_{WW}\phi_{WW} + A_W\phi_{WW} + A_E\phi_E \\ & + A_{EE}\phi_{EE} - A_P\phi_P + S_h = 0 \end{aligned} \tag{27}$$

with

$$S_h = A_P\phi_P^* - A_{WW}\phi_{WW}^* - A_W\phi_W^* - A_E\phi_E^* - A_{EE}\phi_{EE}^*.$$

This local particular solution method can be used for any difference scheme to treat the source term. Comparing this method with the conventional finite difference treatment of source term, whose exact value at the computational location is specified,

$$S_h = S_i, \tag{28}$$

where S_i denotes the source function evaluated at $x = x_i$. The local particular solution method provides a modified

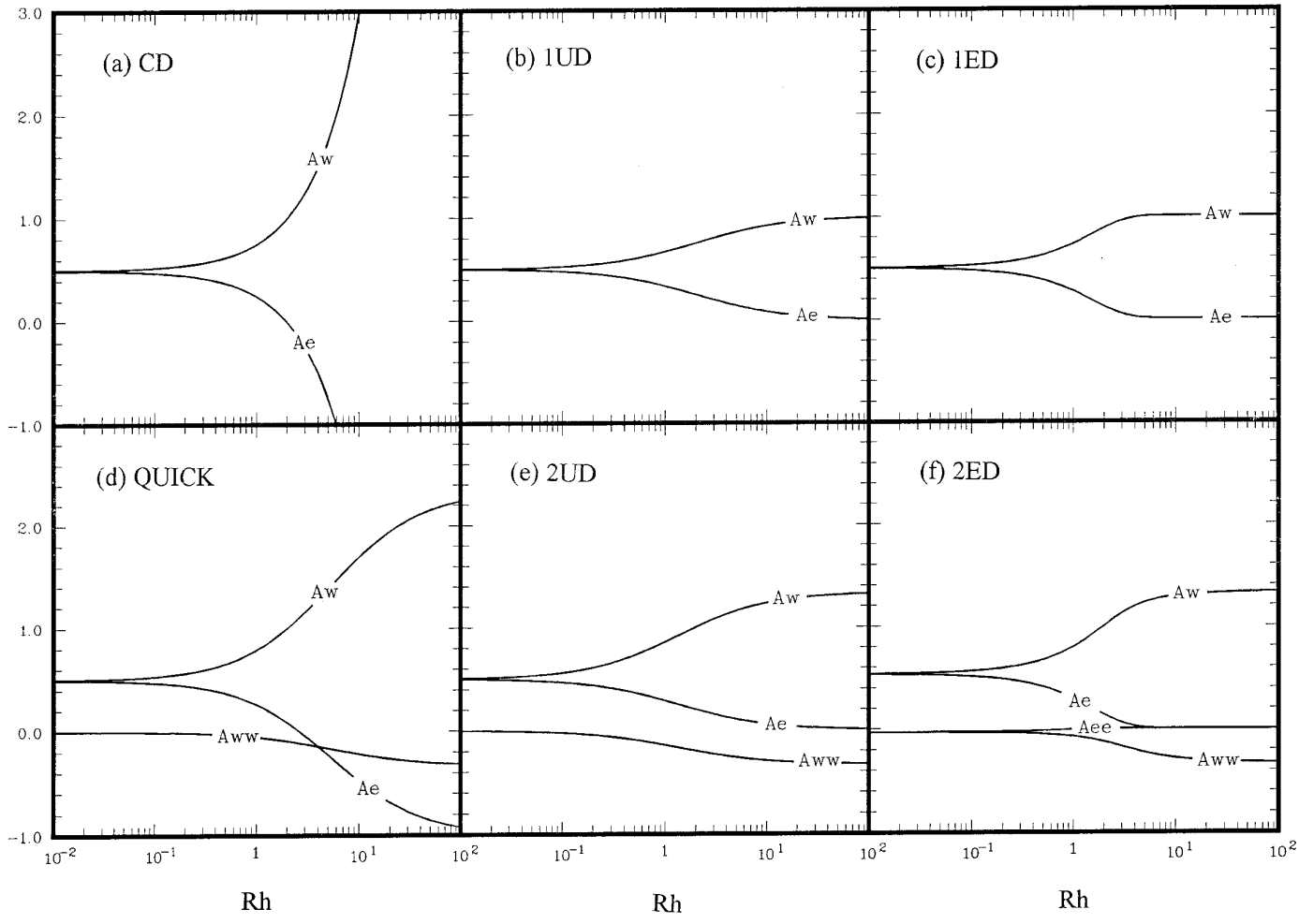

FIG. 3. Influence coefficients for one-dimensional difference schemes.

treatment considering the solution variation in the finite computational cell due to the existence of a source term. In a finite volume procedure, the conventional treatment in Eq. (28) implies an assumed piecewise constant distribution for the source term. Therefore, the present treatment can increase the accuracy of difference expression for the source term.

The above derivation raises the question how to determine a local particular solution to Eq. (24). For an explicitly defined function of the source term, any procedure to find the unconstrained particular solution to the differential equations can be implemented [31]. In the present work, we employ an approximate polynomial fitting procedure of the source term to find a general local particular solution,

$$S(x) = \sum_{n=0}^{N} s_n (x - x_P)^n + \text{HOT} \tag{29}$$

with

$$s_n = \frac{S^{(n)}(x_P)}{n!},$$

where x_P is the coordinate of the location where the Taylor-series expansion (29) is applied and $S^{(n)}$ stands for $d^n S/dx^n$. Substituting Eq. (29) into Eq. (24), neglecting higher-order terms, and assuming that the local particular solution has the form

$$\phi^* = \sum_{n=1}^{N+1} \beta_n (x - x_P)^n, \tag{30}$$

we can obtain the resulting local particular solution by direct comparison of the polynomial coefficients

$$\beta_n = \frac{1}{Rn!} \sum_{m=0}^{N-n+1} \frac{S^{(n+m-1)}}{R^m} \tag{31}$$

or

$$\phi^* = \sum_{n=1}^{N+1} \left[\frac{1}{Rn!} \left(\sum_{m=0}^{N-n+1} \frac{S^{(n+m-1)}}{R^m} \right) (x - x_P)^n \right]$$

and the discretized expression for the extra source term is

$$S_h = -\sum_{n=1}^{N+1} [A_{WW}(-2)^n + A_W(-1)^n + A_E + A_{EE}(2)^n] \beta_n h^n. \quad (32)$$

The terms in the bracket are also identical to those in the TSTE of Eq. (3). Therefore, for any at least first-order accurate scheme, the piecewise constant approximation will yield the same expression as in the conventional formulation Eq. (28). On the other hand, for a second-order difference scheme, the constant approximation Eq. (28) will also achieve the same accuracy as that obtained using piecewise linear approximation for the source term. However, for a first-order difference representation, the piecewise linear approximation will yield higher accuracy than that resulting from the piecewise constant approximation.

The above derivation is proposed for an explicitly defined source term. If the source term in Eq. (23) is not explicitly defined but only obtainable at discrete computational locations, the above modification is also feasible by assigning the coefficients in the approximating polynomial Eq. (29) so that the values of the polynomials at the computational locations equal the prescribed values. For a three-point finite difference stencil considered in the present study, a quadratic polynomial will yield at least a third-order accurate approximation for the source term.

4. TWO-DIMENSIONAL ANALYSIS

The steady two-dimensional convection–diffusion equation considered in the present study has the form

$$L(\Phi) = -u \frac{d\Phi}{dx} - v \frac{d\Phi}{dy} + \frac{d^2\Phi}{dx^2} + \frac{d^2\Phi}{dy^2}, \quad (33)$$

where u and v are the nondimensional velocity components in the x- and y-directions, respectively. Without loss of generality, these velocity components are assumed to be positive. The corresponding computational module for a typical computational point P is given in Fig. 4. Conventional treatment for this two-dimensional problem is based on the combination of two split one-dimensional ones,

$$L_h(\phi) = L_h^x(\phi) + L_h^y(\phi), \quad (34)$$

where $L_h^x(\phi)$ and $L_h^y(\phi)$ are the respective difference expressions for the split convection–diffusion operator in each coordinate direction,

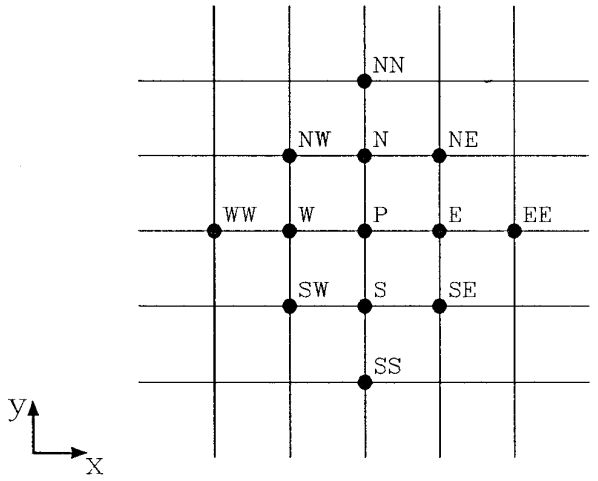

FIG. 4. Computational module for two-dimensional analysis.

$$L^x(\Phi) = -u \frac{d\Phi}{dx} + \frac{d^2\Phi}{dx^2}, \quad L^y(\Phi) = -v \frac{d\Phi}{dy} + \frac{d^2\Phi}{dy^2}. \quad (35)$$

The difference expressions, $L_h^x(\phi)$ and $L_h^y(\phi)$, are the same as the one-dimensional ones given in the previous section. For the exponential schemes considered in the present work, the 1ED scheme can provide the exact solution in the one-dimensional situation. However, in the two-dimensional case, combining two split one-dimensional 1ED schemes yields severe numerical diffusion. The numerical diffusivity in the two-dimensional problem is defined as the one normal to the streamline direction. For example, the numerical diffusivity for the 1UD scheme has been derived by Davies and Mallinson [32],

$$\tau_N = \frac{|V| h \sin(2\theta)}{4(\cos^3\theta + \sin^3\theta)}, \quad (36)$$

where $|V|$ is the magnitude of velocity vector, h is the grid spacing in both directions, and θ is the angle between the velocity vector and the grid line, which can be regarded as the flow skew angle. This expression was also verified numerically by Wolfshtein [33]. In the present work, we will propose novel two-dimensional exponential schemes by minimizing the numerical diffusion.

4.1. *The Nonskew Exponential Scheme (ED)*

Considering the computational module shown in Fig. 4, the approximate solution for Eq. (33) is expressed as

$$\phi(x, y) = \phi_1(x, y) + \phi_2(x, y) + \phi_3(x, y) + \phi_4(x, y) \quad (37a)$$

with the boundary conditions

$$\begin{aligned}
&\phi_1(x,k) = \phi_1(x,-k) = \phi_1(h,y) = 0, \quad && \phi_1(-h,0) = 1,\\
&\phi_2(x,k) = \phi_2(x,-k) = \phi_2(-h,y) = 0, && \phi_2(h,0) = 1,\\
&\phi_3(h,y) = \phi_3(-h,y) = \phi_3(x,k) = 0, && \phi_3(0,-k) = 1,\\
&\phi_4(h,y) = \phi_4(-h,y) = \phi_4(x,-k) = 0, && \phi_4(0,k) = 1,
\end{aligned} \tag{37b}$$

where h and k are the grid spacings in x- and y-directions, respectively. Equation (37) is valid because of the superposition for linear differential equations. All the split solutions, $\phi_1(x, y)$, $\phi_2(x, y)$, $\phi_3(x, y)$, and $\phi_4(x, y)$, satisfy the original differential equation (33). The influence coefficients in the difference equation can be related to these split solutions,

$$\begin{aligned}
A_W &\propto \phi_1(0,0), \quad A_E \propto \phi_2(0,0),\\
A_S &\propto \phi_3(0,0), \quad A_N \propto \phi_4(0,0),
\end{aligned} \tag{38}$$

where $\propto$ is the proportional constant and the difference equation to approximate the two-dimensional convection–diffusion problem will become

$$A_W\phi_W + A_E\phi_E + A_S\phi_S + A_N\phi_N - A_P\phi_P = 0. \tag{39}$$

Consideration of the constant reference mode in this problem provides a further relation between the influence coefficients,

$$A_P = A_W + A_E + A_S + A_N. \tag{40}$$

By separation of variables, we can find the general solutions for these split equations,

$$\begin{aligned}
\phi_1(x,y) &= \sum_{n=1}^{\infty} a_n \exp\left(\frac{ux+vy}{2}\right) \sinh\left[\frac{\sqrt{u^2+v^2+n^2\pi^2/k^2}}{2}(x-h)\right] \sin\left[\frac{n\pi}{2k}(y-k)\right]\\
\phi_2(x,y) &= \sum_{n=1}^{\infty} b_n \exp\left(\frac{ux+vy}{2}\right) \sinh\left[\frac{\sqrt{u^2+v^2+n^2\pi^2/k^2}}{2}(x+h)\right] \sin\left[\frac{n\pi}{2k}(k-y)\right]
\end{aligned} \tag{41}$$

$$\phi_3(x,y) = \sum_{n=1}^{\infty} c_n \exp\left(\frac{ux+vy}{2}\right) \sinh\left[\frac{\sqrt{u^2+v^2+n^2\pi^2/h^2}}{2}(y-k)\right] \sin\left[\frac{n\pi}{2k}(x-h)\right]$$

$$\phi_4(x,y) = \sum_{n=1}^{\infty} d_n \exp\left(\frac{ux+vy}{2}\right) \sinh\left[\frac{\sqrt{u^2+v^2+n^2\pi^2/h^2}}{2}(y+k)\right] \sin\left[\frac{n\pi}{2h}(h-x),\right]$$

with the following constraints:

$$\begin{aligned}
1 &= \sum_{n=1}^{\infty} a_n \exp\left(-\frac{uh}{2}\right) \sinh[\sqrt{(uh)^2+(vh)^2+n^2\pi^2h^2/k^2}] \sin\left[\frac{n\pi}{2}\right],\\
1 &= \sum_{n=1}^{\infty} b_n \exp\left(\frac{uh}{2}\right) \sinh[\sqrt{(uh)^2+(vh)^2+n^2\pi^2h^2/k^2}] \sin\left[\frac{n\pi}{2}\right]\\
1 &= \sum_{n=1}^{\infty} c_n \exp\left(-\frac{vk}{2}\right) \sinh[\sqrt{(uk)^2+(vk)^2+n^2\pi^2k^2/h^2}] \sin\left[\frac{n\pi}{2}\right]\\
1 &= \sum_{n=1}^{\infty} d_n \exp\left(\frac{vk}{2}\right) \sinh[\sqrt{(uk)^2+(vk)^2+n^2\pi^2k^2/h^2}] \sin\left[\frac{n\pi}{2}\right].
\end{aligned} \tag{42}$$

The influence coefficients can then be determined if the series constants a_n, b_n, c_n, and d_n are obtained. However, the constraints in Eq. (42) are not sufficient to yield the complete split solutions. There is only one constraint defined at one computational location for each split solution. More information will be needed to determine the series coefficients, a_n, b_n, c_n, and d_n, i.e., some prescribed distribution along the boundaries of the computational cell. For example, the profile along SW-W-NW in Fig. 4 must be specified to determine $\phi_1(x, y)$. As mentioned in the Introduction, some researchers adopted various assumed distributions based on the values at the computational locations to circumvent this difficulty. In the present study, we adopt a different point of view to treat the series coefficients. We do not assume any explicit distribution but assert that identical distributions along these boundaries should exist. That is,

$$\phi_1(-h,y) = \phi_2(h,y), \quad \phi_3(x,-k) = \phi_4(x,k). \tag{43}$$

This is a direct consequence of a reasonable continuous

boundary profile between two adjacent computational cells. For example, the distribution at SW-W-NW in Fig. 4 should be the same for the two computational cells located at points P and WW. Based on this understanding, the constraints in the split solutions given in Eq. (42) will satisfy the relations

$$\begin{aligned} a_n \exp\left(-\frac{uh}{2}\right) &= b_n \exp\left(\frac{uh}{2}\right), \\ c_n \exp\left(-\frac{vk}{2}\right) &= d_n \exp\left(\frac{vk}{2}\right) \end{aligned} \tag{44}$$

for all possible n. Thus, the corresponding relations for the influence coefficients can be derived from Eqs. (38) and (41),

$$\begin{aligned} A_{\mathrm{W}} &= \alpha_1 \exp\left(\frac{uh}{2}\right), \quad A_{\mathrm{E}} = \alpha_1 \exp\left(-\frac{uh}{2}\right) \\ A_S &= \alpha_2 \exp\left(\frac{vk}{2}\right), \quad A_N = \alpha_2 \exp\left(-\frac{vk}{2}\right). \end{aligned} \tag{45}$$

These relations can be regarded as the two-dimensional extension of the one-dimensional situation given in Eq. (8). The upwind nature of the convection process is automatically considered in this general relation for influence coefficients.

The constants in Eq. (45) are then derived from the requirement of first-order accuracy, which also implies elimination of the spurious velocity:

$$(A_{\mathrm{E}} - A_{\mathrm{W}})h + u = 0, \quad (A_{\mathrm{N}} - A_{\mathrm{S}})k + v = 0. \tag{46}$$

Consequently, the influence coefficients for the first-order accurate nonskew two-dimensional exponential scheme are

$$\begin{aligned} A_{\mathrm{W}} &= \frac{u \exp(uh/2)}{2h \sinh(uh/2)}, \quad A_{\mathrm{E}} = \frac{u \exp(-uh/2)}{2h \sinh(uh/2)}, \\ A_{\mathrm{S}} &= \frac{v \exp(vk/2)}{2k \sinh(vk/2)}, \quad A_N = \frac{v \exp(-vk/2)}{2k \sinh(vk/2)}. \end{aligned} \tag{47}$$

These expressions are identical with those derived from the conventional split one-dimensional analysis.

4.2. *The Skew Exponential Difference Scheme* (*SKED*)

Based on the numerical diffusion analysis [32], we can find that the nonskew exponential scheme (ED) produces severe numerical diffusion. To alleviate this deficiency, the corner computational points (SW, SE, NE, and NW in Fig. 4) should be included in the difference equation. This consideration has been proven to be useful to reduce the numerical diffusion produced in the upwind difference scheme [19]. Thus, the discretized equation assumes the form:

$$\begin{aligned} L_h(\phi) = {} & A_{\mathrm{W}}\phi_{\mathrm{W}} + A_{\mathrm{E}}\phi_{\mathrm{E}} + A_{\mathrm{S}}\phi_{\mathrm{S}} + A_{\mathrm{N}}\phi_{\mathrm{N}} \\ & + A_{\mathrm{SW}}\phi_{\mathrm{SW}} + A_{\mathrm{SE}}\phi_{\mathrm{SE}} + A_{\mathrm{NE}}\phi_{\mathrm{NE}} \\ & + A_{\mathrm{NW}}\phi_{\mathrm{NW}} - A_{\mathrm{P}}\phi_{\mathrm{P}} = 0. \end{aligned} \tag{48}$$

The Taylor-series expansion of this discretized equation can be expressed as

$$\begin{aligned} L_h(\Phi_h) = {} & (-A_{\mathrm{W}} + A_{\mathrm{E}} - A_{\mathrm{SW}} + A_{\mathrm{SE}} + A_{\mathrm{NE}} - A_{\mathrm{NW}})h \frac{\partial \Phi}{\partial x} \\ & + (-A_{\mathrm{S}} + A_{\mathrm{N}} - A_{\mathrm{SW}} - A_{\mathrm{SE}} + A_{\mathrm{NE}} + A_{\mathrm{NW}})k \frac{\partial \Phi}{\partial y} \\ & + (A_{\mathrm{W}} + A_{\mathrm{E}} + A_{\mathrm{SW}} + A_{\mathrm{SE}} + A_{\mathrm{NE}} + A_{\mathrm{NW}}) \frac{h^2}{2} \frac{\partial^2 \Phi}{\partial x^2} \\ & + (A_{\mathrm{SW}} - A_{\mathrm{SE}} + A_{\mathrm{NE}} - A_{\mathrm{NW}})hk \frac{\partial^2 \Phi}{\partial x \partial y} \\ & + (A_{\mathrm{S}} + A_{\mathrm{N}} + A_{\mathrm{SW}} + A_{\mathrm{SE}} + A_{\mathrm{NE}} + A_{\mathrm{NW}}) \\ & \frac{k^2}{2} \frac{\partial^2 \Phi}{\partial y^2} + \mathrm{HOT}. \end{aligned} \tag{49}$$

Performing an analysis similar to that for the nonskew exponential difference scheme yields the values of the influence coefficients in the skew scheme,

$$\begin{aligned} A_{\mathrm{W}} &= \alpha_1 \exp\left(\frac{uh}{2}\right), \quad A_{\mathrm{E}} = \alpha_1 \exp\left(-\frac{uh}{2}\right), \\ A_{\mathrm{S}} &= \alpha_2 \exp\left(\frac{vk}{2}\right), \quad A_{\mathrm{N}} = \alpha_2 \exp\left(-\frac{vk}{2}\right) \\ A_{\mathrm{SW}} &= \alpha_3 \exp\left(\frac{uh + vk}{2}\right), \quad A_{\mathrm{SE}} = \alpha_3 \exp\left(\frac{-uh + vk}{2}\right), \\ A_{\mathrm{NE}} &= \alpha_3 \exp\left(-\frac{uh + vk}{2}\right), \\ A_{\mathrm{NW}} &= \alpha_3 \exp\left(\frac{uh - vk}{2}\right), \end{aligned} \tag{50}$$

where α_1 and α_2 are called normal constants and α_3 is called the skew constant. These constants are determined by minimizing the numerical diffusion to yield a more accurate discretization. Comparing this equation with Eq. (45), it is clear that the skew scheme provides a general representation. For the first-order term in TSTE, the fol-

lowing equations must be satisfied for prevention of spurious velocity:

$$\begin{aligned}(-A_W + A_E - A_{SW} + A_{SE} + A_{NE} - A_{NW}) &= -u/h \\ (-A_S + A_N - A_{SW} - A_{SE} + A_{NE} + A_{NW}) &= -v/k.\end{aligned} \tag{51}$$

These constraints are similar to those for the nonskew scheme depicted in Eq. (46). The corresponding equations for the coefficients are

$$\begin{aligned}\alpha_1 + 2\alpha_3 \cosh\left(\frac{vk}{2}\right) &= \frac{u}{2h\sinh(uh/2)} \\ \alpha_2 + 2\alpha_3 \cosh\left(\frac{uh}{2}\right) &= \frac{v}{2k\sinh(vk/2)}.\end{aligned} \tag{52}$$

The other equation needed to find the influence coefficients is based on the evaluation of numerical diffusion. From Eqs. (49), (50) and incorporating Eq. (52), components of the effective diffusivity tensor for the skew exponential scheme can be written as

$$\begin{aligned}\tau_{xx} &= \frac{uh}{2}\coth\left(\frac{uh}{2}\right) \\ \tau_{xy} &= 2hk\alpha_3 \sinh\left(\frac{uh}{2}\right)\sinh\left(\frac{vk}{2}\right) \\ \tau_{yy} &= \frac{vk}{2}\coth\left(\frac{vk}{2}\right),\end{aligned} \tag{53}$$

where τ_{xx} and τ_{yy} are the normal diffusivities and τ_{xy} is the skew diffusivity. Let θ_P be the angle between the principal axis of the diffusivity tensor and the x-axis. The principal diffusivities τ_{XX} and τ_{YY} will satisfy the relations

$$\begin{aligned}\tau_{xx} - \tau_{yy} &= (\tau_{XX} - \tau_{YY})\cos(2\theta_P) \\ \tau_{xy} &= \frac{1}{2}(\tau_{XX} - \tau_{YY})\sin(2\theta_P).\end{aligned} \tag{54}$$

The effective diffusivity, defined as the diffusivity normal to the flow direction, can then be expressed as [34]

$$\tau_{\text{eff}} = \frac{\tau_{XX}\tau_{YY}}{\tau_{XX}\cos^2(\theta - \theta_P) + \tau_{YY}\sin^2(\theta - \theta_P)}. \tag{55}$$

Expanding the above equation and combining it with the relations given in Eq. (54), the effective diffusivity can be expressed in terms of the normal and skew diffusivities,

$$\tau_{\text{eff}} = \frac{\tau_{xx}\tau_{yy} - \tau_{xy}^2}{\tau_{xx}\cos^2\theta + \tau_{yy}\sin^2\theta + \tau_{xy}\sin(2\theta)}. \tag{56}$$

The numerically induced diffusivity is the difference between the effective and the physical diffusivity:

$$\tau_N = \tau_{\text{eff}} - 1 = \frac{\tau_{xx}\tau_{yy} - \tau_{xy}^2}{\tau_{xx}\cos^2\theta + \tau_{yy}\sin^2\theta + \tau_{xy}\sin(2\theta)} - 1. \tag{57}$$

This is a general expression for the numerical diffusivity of difference schemes. With this formulation, we can also find the numerical diffusivity for many existing schemes, such as the nonskew exponential difference scheme (ED), the skew upwind difference scheme (SKUD), and the finite analytic method (FA).

From Eq. (53), it can be found that the normal diffusivities in the x-y coordinates, τ_{xx} and τ_{yy}, are functions of flow velocity and grid spacing, independent of the constants, α_1, α_2, and α_3. Therefore, the numerical diffusivity depends only on α_3, irrespective of α_1 and α_2. A reasonable selection of α_3 is based on the fulfillment of the zero numerical diffusivity condition. From Eq. (57), this selection will lead to the description for the skew diffusivity, τ_{xy},

$$\tau_{xy} = \frac{-\sin(2\theta) + \sqrt{4(\tau_{xx}\tau_{yy} - \tau_{xx}\cos^2\theta - \tau_{yy}\sin^2\theta) + \sin^2(2\theta)}}{2}, \tag{58}$$

and the corresponding scheme constants can be determined with Eqs. (52), (53), and (58):

$$\begin{aligned}\alpha_1 &= \frac{1}{h\sinh(uh/2)}\left[\frac{u}{2} - \frac{\tau_{xy}}{k}\coth\left(\frac{vk}{2}\right)\right] \\ \alpha_2 &= \frac{1}{k\sinh(vk/2)}\left[\frac{v}{2} - \frac{\tau_{xy}}{h}\coth\left(\frac{uh}{2}\right)\right] \\ \alpha_3 &= \frac{\tau_{xy}}{2hk\sinh(uh/2)\sinh(vk/2)}.\end{aligned} \tag{59}$$

From Eqs. (53) and (58), one can easily prove that the skew diffusivity will always be nonnegative since the normal diffusivities are greater than one. The corresponding skew constant α_3 is also nonnegative. However, in some circumstances, one of the normal constants may become negative, which results in a nonmonotonic difference scheme. To ensure monotonicity, this negative normal constant is reset to zero and the other two constants are recalculated from Eq. (52). This procedure can be interpreted to provide the minimum numerical diffusivity required to maintain scheme monotonicity. Consequently, scheme constants in this monotonic skew difference representation can be summarized as

$$\alpha_3 = \min\left(\frac{\tau_{xy}}{2h\sinh\left(\frac{uh}{2}\right)\sinh\left(\frac{vk}{2}\right)}, \frac{u}{4h\sinh\left(\frac{uh}{2}\right)\cosh\left(\frac{vk}{2}\right)}, \frac{v}{4k\sinh\left(\frac{vk}{2}\right)\cosh\left(\frac{uh}{2}\right)}\right) \tag{60}$$

$$\alpha_1 = \frac{u}{2h\sinh(uh/2)} - 2\alpha_3\cosh\left(\frac{vk}{2}\right)$$

$$\alpha_2 = \frac{v}{2k\sinh(vk/2)} - 2\alpha_3\cosh\left(\frac{uh}{2}\right).$$

The last two equations are directly derived from Eq. (52) to ensure elimination of the spurious velocity.

Based on the numerical diffusivity analysis given above, we can derive two kinds of the skew exponential scheme. The first (SKED1), given in Eq. (59), is completely free of numerical diffusivity but may induce spurious oscillation. The second (SKED2), shown in Eq. (60), gives a monotonic scheme with minimum numerical diffusivity. In a later section, we will blend these two schemes to provide a more accurate and monotonic scheme. This blended scheme may allow negative influence coefficients if the monotonicity in the solution is still preserved.

4.3. *Numerical Diffusivity*

For comparison purposes, we calculate the numerical diffusivities of some widely used schemes. These schemes include the nonskew exponential difference scheme (ED), the skew upwind difference scheme (SKUD), and the finite analytic method (FA). These schemes are only first-order accurate in a one-dimensional situation based on TSTE analysis. All the second-order accurate schemes, on the other hand, will not produce numerical diffusion but may result in a spurious oscillatory solution. All the analyses given herein are based on Taylor-series expansion, Eq. (49), and the numerical diffusivity, Eq. (57), if the influence coefficients are given. The influence coefficients for SKUD and FA can be found in the existing literature [19, 28]. The resulting numerical diffusivities are listed in Table I.

Representative influence coefficients and numerical diffusivities for the two-dimensional schemes considered in the present work are calculated and illustrated in Figs. 5.1–5.5 Grid spacings in the x- and y-directions for these calculations are set to be equal ($h = k$) and the cell Reynolds number ranges from 0 to 100. The influence coefficients have been normalized by their diagonal term. Only A_W and A_{SW} are given in these figures since other coefficients can be easily derived from the symmetric condition. The numerical diffusivity has also been normalized by the resulting cell Reynolds number:

$$T_d = \tau_N/|V|h. \tag{61}$$

From these figures, one can find that the influence coefficients of ED, FA, and SKED2 are all-positive, which is the requirement for a monotonic difference scheme. The possible oscillatory schemes, SKUD and SKED1, possess negative influence coefficients. In some circumstances, these two schemes may also yield monotonic solution if the diffusion transport is significant. As for the numerical diffusivity, the ED scheme gives the largest numerical diffusivity and SKUD may yield negative numerical diffusivity. Among the monotonic schemes, the SKED2 scheme yields the smallest numerical diffusivity. This is also the minimum numerical diffusion required to prevent the problem of an unbounded solution. The FA method, despite the larger amount of computational effort required, is worse than the simpler SKED2, especially when the velocity vector is close to the grid diagonal line ($\theta = 45°$). Therefore, SKED1 and SKED2 are superior to SKUD, ED, and FA, in view of the inherent numerical diffusion and scheme monotonicity. Meanwhile, if the physical diffusion is significant in some flow region, these two schemes will be identical and yield the monotonic scheme without numerical diffusion. Figure 6 illustrates the range of cell Reynolds numbers that ensure monotonic behavior for SKED and SKUD in terms of the flow skew angle, θ. It is shown that SKED may give both accurate and monotonic solutions if the cell Reynolds number is not larger than 8. This critical cell Reynolds number increases with the flow skew angle. As for SKUD, the critical cell Reynolds number will reach a minimum value of about 4, corresponding to a flow skew angle $\theta = \tan^{-1}(v/u) = \tan^{-1}(1/2)$ or $\theta = \tan^{-1}(2)$.

5. NUMERICAL EXPERIMENTS

The difference approximations for the convection–diffusion equation can be evaluated by solving several test problems. Both one- and two-dimensional problems are examined with the proposed schemes and the results compared with those from other existing difference approximations. For the one-dimensional situation, the schemes examined include the first-order upwind difference (1UD), central difference (CD), first-order exponential difference (1ED), quadratic upstream interpolation for convective kinematics (QUICK), second-order upwind difference (2UD), and the second-order exponential difference (2ED). The last scheme is the novel one proposed herein. The effects of source term on scheme accuracy are also investigated and the local particular solution method is

TABLE I

Numerical Diffusivities of Difference Schemes

Scheme	Γ_N
ED	$\dfrac{\lvert V\rvert hk\sin(2\theta)\coth(uh/2)\coth(vk/2)}{h\cos^3(\theta)\coth(uh/2)+k\sin^3(\theta)\coth(vk/2)}-1$
	$\dfrac{16/\lvert V\rvert+8h\cos(\theta)+8k\sin(\theta)+2\lvert V\rvert hk\sin(2\theta)-9\lvert V\rvert h^2\sin^2(\theta)}{8h\cos^3(\theta)+8k\sin^3(\theta)+12h\sin(\theta)\sin(2\theta)+16/\lvert V\rvert}-1 \quad \text{for } uk>2vh$
SKUD	$\dfrac{16/\lvert V\rvert+8h\cos(\theta)+8k\sin(\theta)+2\lvert V\rvert hk\sin(2\theta)-9\lvert V\rvert[h\sin(\theta)+k\cos(\theta)]^2}{8h\cos^3(\theta)+8k\sin^3(\theta)+[h\sin(\theta)+k\cos(\theta)]\sin(2\theta)+16/\lvert V\rvert}-1 \quad \text{for } 4vh\geq 2uk>vh$
	$\dfrac{16/\lvert V\rvert+8h\cos(\theta)+8k\sin(\theta)+2\lvert V\rvert hk\sin(2\theta)-9\lvert V\rvert k^2\cos^2(\theta)}{8h\cos^3(\theta)+8k\sin^3(\theta)+12k\cos(\theta)\sin(2\theta)+16/\lvert V\rvert}-1 \quad \text{for } vh\geq 2uk$
FA	$\dfrac{\lvert V\rvert hk\sin(2\theta)\coth(uh/2)\coth(vk/2)-2\lvert V\rvert\{\sin(\theta)(1-P_A-P_B)/(1-P_B)/[k\coth(uh/2)]\}^2}{4h\cos^3(\theta)\coth(uh/2)+4k\sin^3(\theta)\coth(vk/2)+4\sin(\theta)\sin(2\theta)(1-P_A-P_B)/(1-p_B)/[k\coth(uh/2)]}-1$
SKED1	0
SKED2	$\dfrac{\lvert V\rvert hk\sin(2\theta)\coth(uh/2)\coth(vk/2)-32\alpha_3^2h^2k^2\sinh^2(uh/2)\sinh^2(vk/2)/\lvert V\rvert}{4h\cos^3(\theta)\coth(uh/2)+4k\sin^3(\theta)\coth(vk/2)+16\alpha_3hk\sinh(uh/2)\sinh(vk/2)\sin(2\theta)}-1$

Note. $P_A = 2uh\cosh(uh/2)\cosh(vk/2)\coth(uh/2)E$; $P_B = 1+(P_A-1)vh\coth(vk/2)/[uk\cosh(uh/2)]$; $E=\sum_{m=1}^{\infty}-1(-1)^m\lambda_m h/[(uh/2)^2+(\lambda_m h)^2]\cosh\sqrt{[(uh/2)^2+(vk/2)^2]k^2}$; $\lambda_m=((2m-1)/2)\pi$.

used to raise the accuracy of first-order schemes (1UD and 1ED).

For the two-dimensional test problems, the difference schemes examined include the schemes based on one-dimensional analysis, except CD which has been proven to be unsuitable for high Reynolds number flow calculations, and those based on two-dimensional analysis. The schemes based on two-dimensional analysis include the skew upwind difference (SKUD), finite analytical method (FA), and the skew exponential schemes (SKED1 and SKED2). The last two schemes are proposed in the present study. The one-dimensional difference schemes are applied in the two split directions to obtain the resulting difference expressions. Finally, a stable scheme combining the special features of SKED1 and SKED2 is proposed to yield a more accurate method. This scheme is based on the idea that the numerical diffusion should be controlled and introduced to the scheme only when it is truly needed. All the

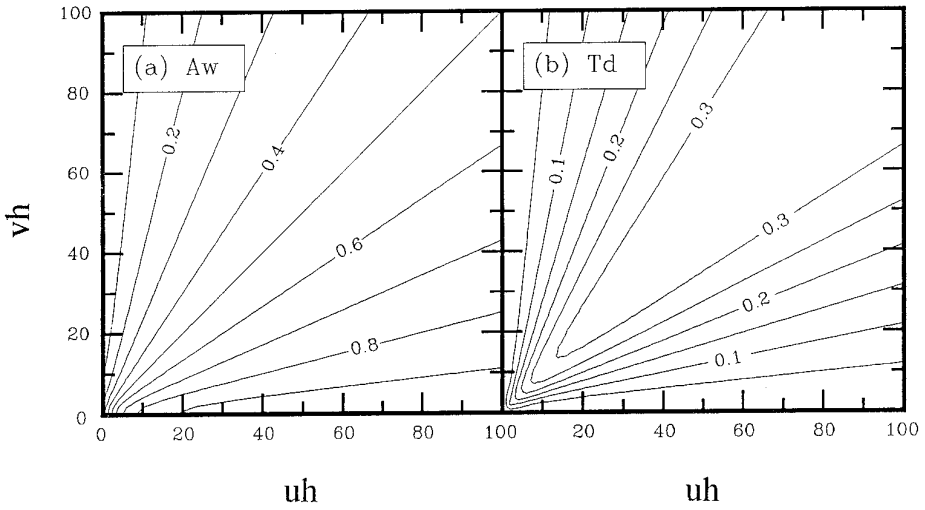

FIG. 5.1. Influence coefficients and numerical diffusivity for ED.

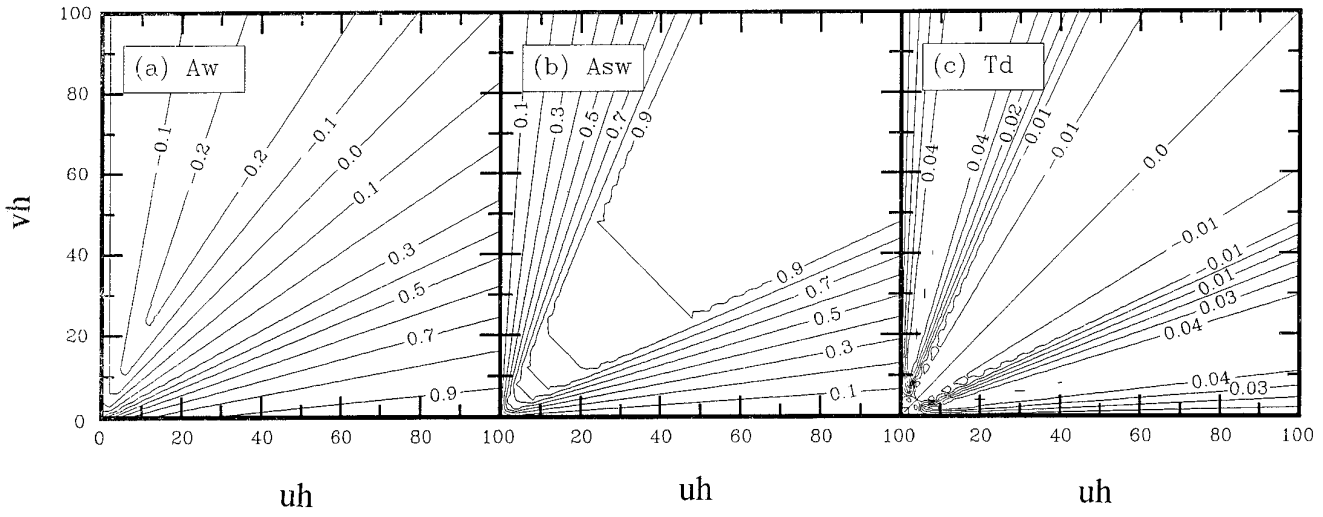

FIG. 5.2. Influence coefficients and numerical diffusivity for SKUD.

computational results support our analyses in previous sections.

5.1. *One-Dimensional Problems*

5.1.1. A Problem with a Quadratic Source Term. The first test problem considered is the convection–diffusion equation with a quadratically distributed source term,

$$R\frac{d\Phi}{dx} = \frac{d^2\Phi}{dx^2} + S_0 + S_1 x + S_2 x^2, \tag{62}$$

with the boundary conditions,

$$\Phi(0) = 0.0, \quad \Phi(1) = 1.0.$$

The exact solution for this problem is:

$$\Phi(x) = [1 - \Phi_P(1)]\frac{\exp(Rx) - 1}{\exp(R) - 1} + \Phi_P(x) \tag{63}$$

and the particular solution $\Phi_P(x)$, due to the existence of the source term is

$$\Phi_P(x) = \left(\frac{2S_2}{R^3} + \frac{S_1}{R^2} + \frac{S_0}{R}\right)x + \left(\frac{S_2}{R^2} + \frac{S_1}{2R}\right)x^2 + \left(\frac{S_2}{3R}\right)x^3.$$

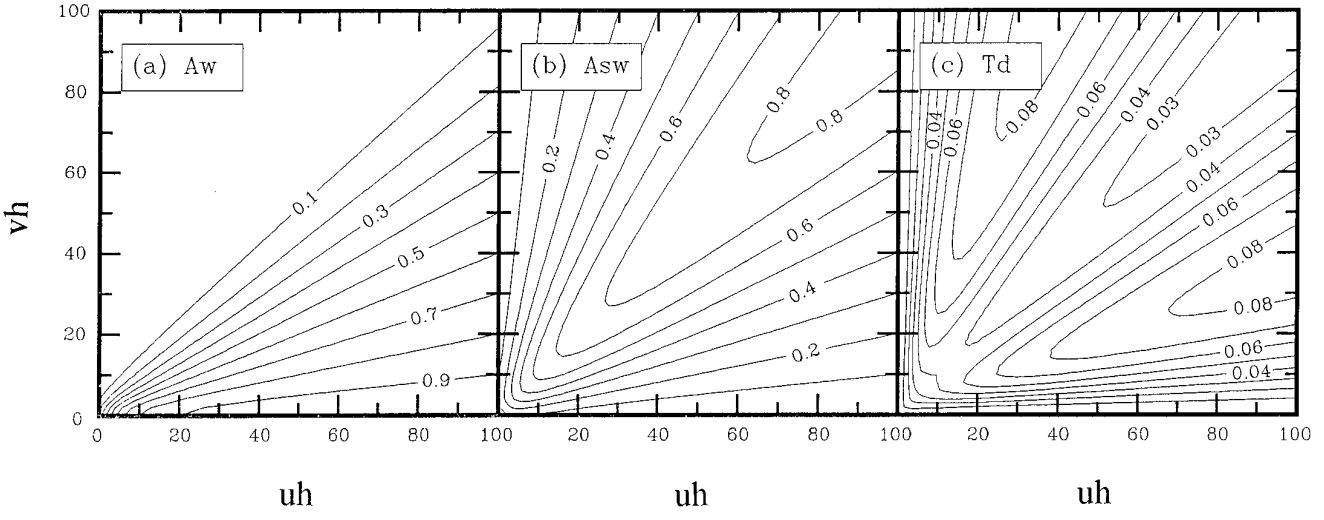

FIG. 5.3. Influence coefficients and numerical diffusivity for FA.

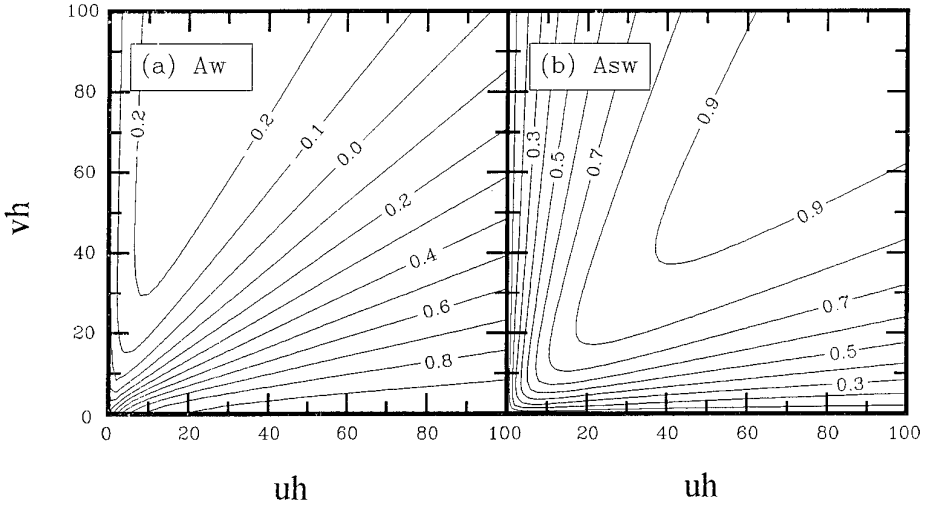

FIG. 5.4. Influence coefficients and numerical diffusivity for SKED1.

The corresponding difference equation can be expressed as Eq. (2) and the system equations are solved by a general pentadiagonal matrix algorithm (PDMA) [12]. The starting problem for the 5-point stencil schemes (2UD, QUICK, and 2ED) are solved by incorporating the 1UD scheme to provide the difference equation for the computational node nearest the upstream boundary.

Figure 7.1 shows the maximum nodal error of the computational results by various difference schemes for the special case of no extra source term ($S_0 = S_1 = S_2 = 0$). The flow Reynolds number is 500 and the grid spacing is set to have the cell Reynolds number ranging from 0.01 to 100. For the high Reynolds number flow, a thin boundary layer will be established at the downstream boundary ($x =$ 1). Schemes with negative characteristic roots (CD and QUICK) will yield oscillatory solutions if the cell Reynolds number exceeds their critical values. Therefore, even though these schemes possess high-order accuracy in TSTE analysis, the computational results are not acceptable due to the unphysical wiggle. As the cell Reynolds number falls below their corresponding critical value, these two schemes will predict more accurate results than 1UD. As for our proposed 2ED scheme, the calculated results are quite satisfactory over all Reynolds numbers and grid spacings. Especially for the low cell Reynolds number situation, the 2ED scheme yields a fourth-order accurate difference expression and provides highly accurate results. For high cell Reynolds number condition, the 2ED scheme will be-

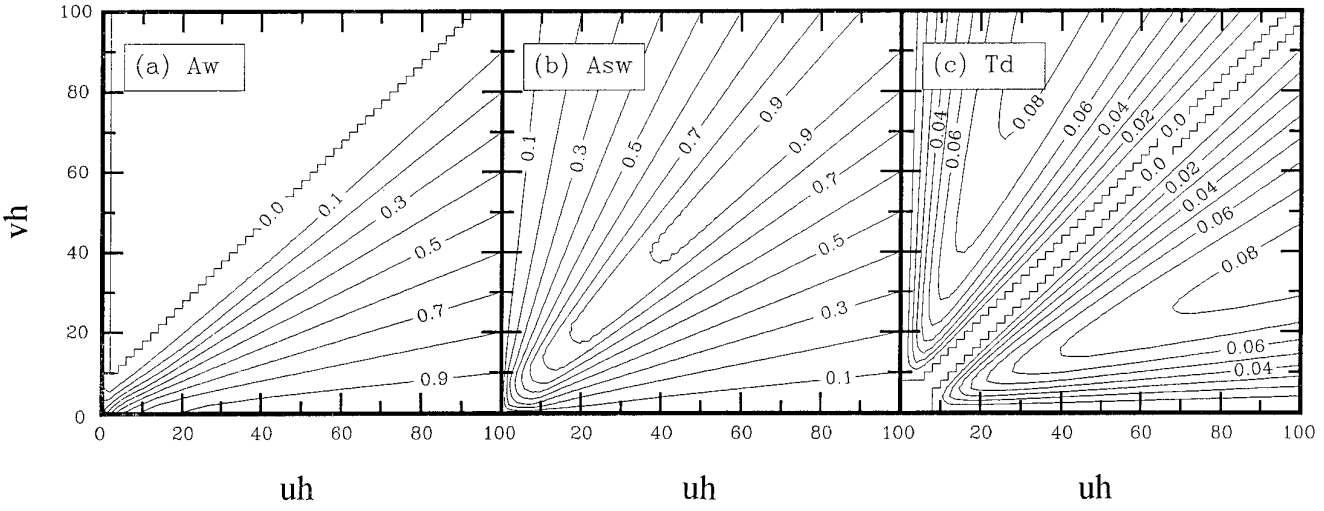

FIG. 5.5. Influence coefficients and numerical diffusivity for SKED2.

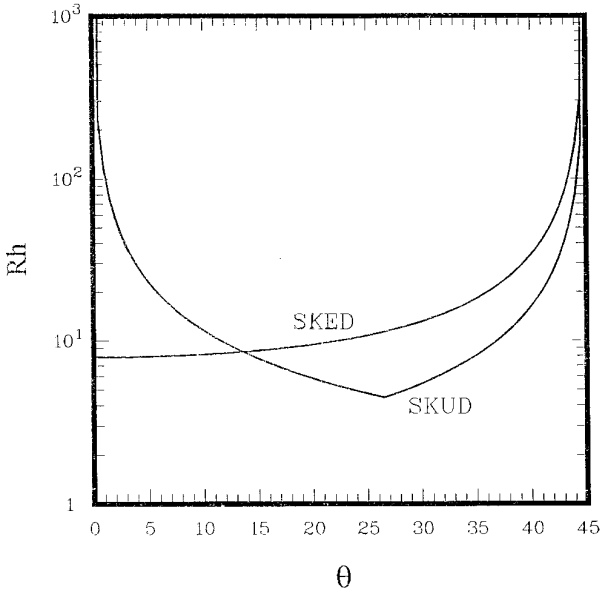

FIG. 6. Critical cell Reynolds numbers for SKUD and SKED.

have like the 2UD scheme since the downstream influence can be neglected and still yields quite accurate results. Therefore, for the source-free convection–diffusion problem, one can conclude that the 1UD scheme gives satisfactory solution only for high Reynolds number situation and will produce large numerical error for low cell Reynolds number flow. Both the CD and QUICK schemes, on the other hand, yield quite accurate solutions if the cell Reynolds number is not larger than their respective critical values. Both the 2ED and 2UD schemes can produce accurate solutions for all cell Reynolds numbers and the former can provide more accurate predictions in diffusion-dominated situations. As shown in the previous analysis, the 1ED will yield exact solutions and no numerical errors can be detected.

The effects of the source term on the solution accuracy are considered by the introduction of a quadratic source term distribution ($S_0 = S_1 = 0$, $S_2 = 4.5R$) and the results are shown in Fig. 7.2. The mode parameter m in this and the following figures is defined as

$$m = N + 1, \tag{64}$$

where N is the approximate order for the source term as given in Eq. (29). That is, $m = 1$ corresponds to the piecewise constant approximation for the source term and $m = 2$ is the piecewise linear approximation. Figure 7.2a represents the mean computational error at computational nodes for the results predicted by various difference schemes with a piecewise constant treatment for the source term ($m = 1$). This treatment is frequently adopted in conventional finite difference approaches. As shown in this figure, the accuracy of the two first-order schemes (1UD and 1ED) has deteriorated; while for the higher order schemes, the accuracy persists, irrespective of the existence of the source term. This phenomenon can be explained through the TSTE analysis given in Section 3. The 1ED scheme, which is an exact difference expression for the source-free problem, will be reduced to a first-order accurate scheme in the high cell Reynolds number situation, as depicted in the TSTE. Figure 7.2(b) shows the mean error that resulted from the piecewise linear approximation for the source term in finding the local particular solution ($m = 2$). The accuracy of 1UD and 1ED increases, especially in the high Reynolds number situation. Figure 7.2c depicts the results based on the quadratic treatment for the source term ($m = 3$). Since the global source term is also of quadratic distribution, this treatment will transform the problem to a source-free convection–diffusion one. No additional numerical error can be found for the 1ED scheme; that is, the accuracy of first-order upwind schemes (1UD and 1ED) is completely recovered with the appropriate treatment of the source term. Therefore, to obtain a reasonable numerical prediction, we can use the 1ED with suitable treatment of the source term (at least piecewise linear approximation) or adopt the 2ED scheme with simple piecewise constant treatment. Figure 7.3 illustrates the effects of adopting a local particular solution method in increasing the scheme accuracy for 1ED and 2ED. From this simple test problem, we can find that the accuracy of 1ED can be raised in the existence of an extra source term. For a high-order scheme such as 2ED, the treatment of the source term is not critical, especially in the low cell Reynolds number region.

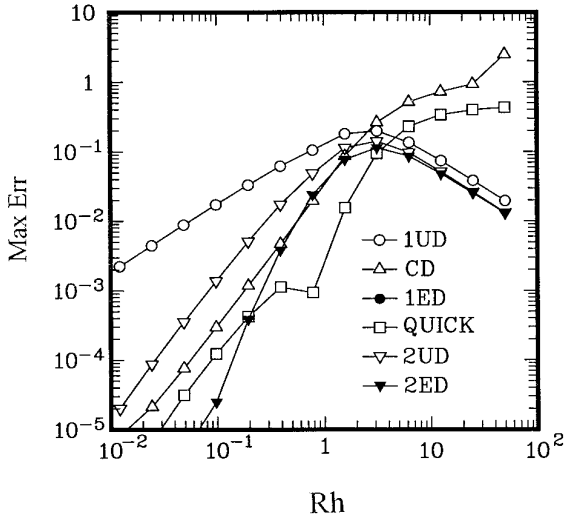

FIG. 7.1. Computational errors without source term.

5.1.2. The Problem with a Piecewise Linear Source

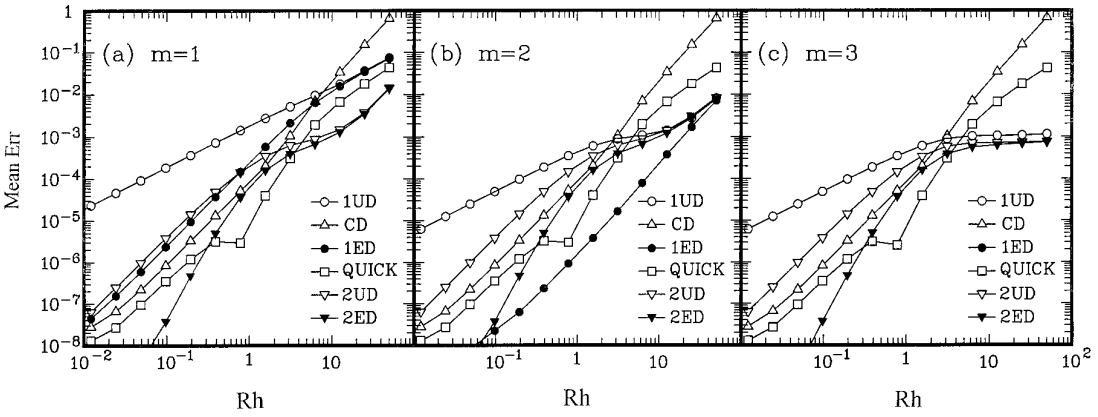

FIG. 7.2. Computational errors with different treatment of source term.

TERM. The second test problem considered in the one-dimensional situation is the high Reynolds number flow with a piecewise linear source. This problem was raised and extensively studied by Leonard [7],

$$R\frac{d\Phi}{dx} = \frac{d^2\Phi}{dx^2} + S, \tag{65}$$

with the following boundary conditions:

$$\Phi(0) = \Phi(1) = 0.$$

The source term is a piecewise linear distribution with the expression

$$S(x) = ax + b$$

$$= -\frac{ax_1 + b}{x_2}x + \frac{x_1 + x_2}{x_2}(ax_1 + b) \tag{66}$$

$$= 0$$

for $0 \le x < x_1$

for $x_1 \le x < x_1 + x_2$

for $x_1 + x_2 \le x$.

The corresponding exact solution can be easily found with some simple algebra. In the present study, the computational parameters are taken,

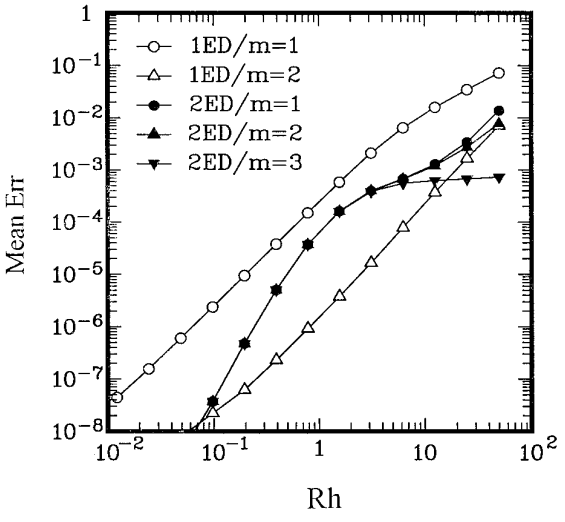

FIG. 7.3. Effects of local approximation for source term.

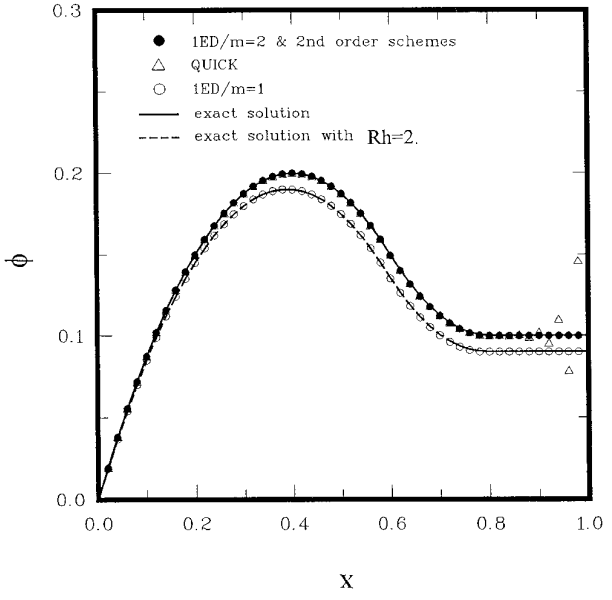

FIG. 8. Computational results for a problem with piecewise linear source term.

$$a = -2.5R, \quad b = 1.0R, \quad x_1 = 0.6, \quad x_2 = 0.2, \quad (67)$$

and the flow Reynolds number is $R = 10^6$ with the grid spacing $h = \frac{1}{50}$. The computational results for this problem are shown in Fig. 8. All the stable higher-order schemes (2UD and 2ED), as well as the 1ED scheme with piecewise linear approximation ($m = 2$) for the source term, give very accurate solutions. The QUICK scheme, on the other hand, displays some severe oscillatory behavior near the downstream boundary. The 1ED scheme with inappropriate treatment of the source term ($m = 1$) yields a distribution corresponding to an effective cell Reynolds number $Rh = 2$. This phenomenon is due to the huge numerical diffusion ($Rh/2$) inherent in the first-order scheme which can be derived from the TSTE analysis [7].

5.2. *Two-Dimensional Problems*

Performances of difference schemes are demonstrated by solving a scalar transport problem in a two-dimensional constant velocity field,

$$u\frac{\partial \Phi}{\partial x} + v\frac{\partial \Phi}{\partial y} = \mu\left(\frac{\partial^2 \Phi}{\partial x^2} + \frac{\partial^2 \Phi}{\partial y^2}\right), \quad (68)$$

where u and v are the constant velocity components and assumed to be positive, μ is the fluid diffusivity. A uniform grid spacing, $h = \frac{1}{40}$, is assigned for both the x and y directions in the computational region $0 \le x \le 1$ and $0 \le y \le 1$. The cell Reynolds numbers in x- and y-directions, $R_{x,h}$ and $R_{y,h}$, are defined as

$$R_{x,h} = \frac{uh}{\mu}, \quad R_{y,h} = \frac{vh}{\mu}. \quad (69)$$

The starting problem for the higher-order accurate upwind difference schemes incorporating more computational points (QUICK, 2UD, and 2ED) are solved by using the first-order upwind difference scheme (1UD) at the computational points nearest the upstream boundaries to initialize the solution procedure. The resulting difference equations are then solved iteratively by the simple point-by-point Gauss–Seidel method. The convergence criterion is that the total solution error should be less than 10^{-3}. Tighter criteria are also tested and the results show that this quantity is sufficient to provide convergent solutions. For nonmonotonic schemes, the results must be underrelaxed between two successive computations to prevent divergence due to the lack of diagonal dominance in the coefficient matrix. However, if convection transport problems are considered, there only needs to be a single sweep to obtain the solution for all difference schemes except QUICK, which still requires further iterations, owing to the nonvanishing downstream influence coefficients.

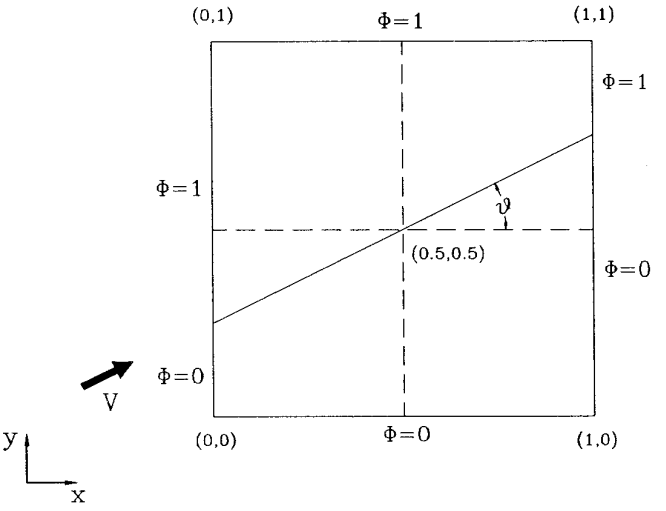

FIG. 9. Computational domain, velocity vector and boundary condition for a two-dimensional test problem.

5.2.1. Convective Transport without Physical Diffusivity. The first problem considered is a convection transport without physical diffusivity ($\mu = 0$). The two cell Reynolds numbers, $R_{x,h}$ and $R_{y,h}$, will become infinity and the solution will depend on the upstream boundary condition only. Figure 9 shows the computational domain, the velocity vector, and the associated boundary conditions. The magnitude of the velocity vector and the flow skew angle are

$$|V| = \sqrt{u^2 + v^2}, \quad \theta = \tan^{-1}(v/u). \quad (70)$$

The exact solution at any constant-x cross section is a step-change distribution. This is a benchmark problem to examine the accuracy of two-dimensional difference schemes [10, 24]. For the difference schemes considered in the present study, the first-order upwind difference (1UD) will be identical with the first-order exponential difference (1ED), the second-order upwind difference (2UD) will be identical with the second-order exponential difference (2ED), and the finite analytical method (FA) will be identical with the monotonic skew exponential difference (SKED2) in this limiting situation. Three flow skew angles are investigated: $\theta = 15°$, $\theta = 30°$, and $\theta = 45°$. The computational results, along with the exact solution at $x = 0.5$, by various difference schemes for these flow skew angles are illustrated in Figs. 10.1–10.3.

The 1UD/1ED and FA/SKED2 schemes are monotonic with all positive influence coefficients and do not produce an oscillatory solution, while the QUICK, 2UD/2ED, SKUD, and SKED1 schemes suffer from a boundedness problem if there exist abrupt changes in the solution profile. Among these oscillatory schemes, the QUICK scheme

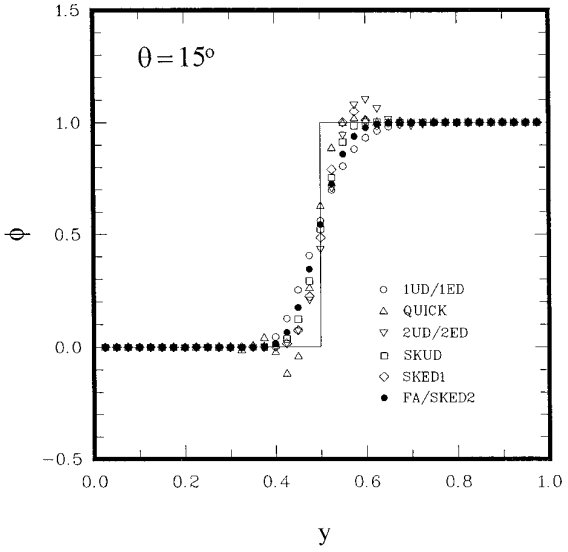

FIG. 10.1. Computational results at $\theta = 15°$.

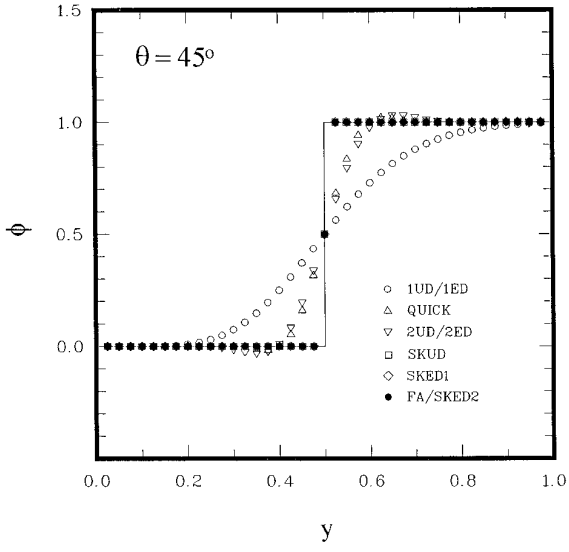

FIG. 10.3. Computational results at $\theta = 45°$.

gives a severe wiggle distribution upstream of the change, while this oscillation happens downstream for the other schemes. This can be attributed to the negative influence coefficients of the downstream neighboring node ($A_e < 0$ shown in Fig. 3) for QUICK.

For other schemes, the negative influence coefficients are mainly associated with the upstream neighboring nodes ($A_{WW} < 0$ for 2UD/2ED shown in Fig. 3 and $A_S < 0$ for SKUD and SKED1 shown in Fig. 5). Therefore, although the 2UD and 2ED schemes possess all positive characteristic roots in the one-dimensional situation, they may nevertheless produce oscillatory solutions in multidimensional calculation. However, this oscillation is confined in the regions around sharp gradients in the solution profile. As for the two-dimensional-based difference schemes (SKUD and SKED1), the oscillation is not significant if the skew angle is not too large ($\theta = 15°$ in Fig. 10.1) or near the grid diagonal line ($\theta = 45°$ in Fig. 10.3). Especially in the case of $\theta = 45°$, all the two-dimensional-based schemes (SKUD, SKED1, and FA/SKED2), which satisfy the shift condition, give the exact solution.

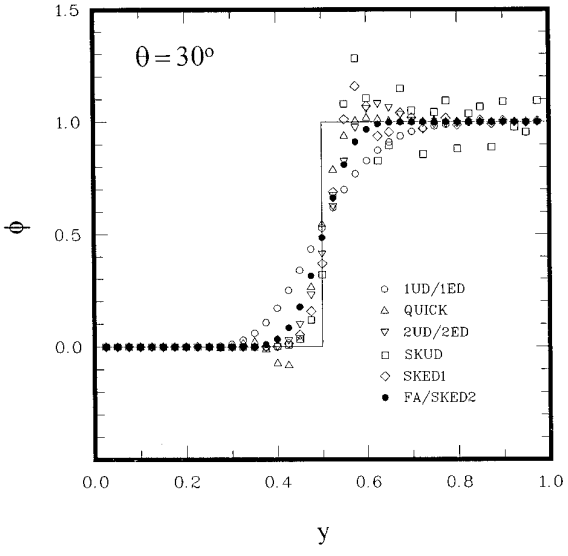

FIG. 10.2. Computational results at $\theta = 30°$.

As shown in Fig. 5, SKUD may yield negative numerical diffusivity if the skew angle is between 25° and 35°. Therefore, at $\theta = 30°$ as shown in Fig. 10.2, the SKUD scheme produces severe oscillatory results downstream of the abrupt change in the solution profile. This wiggle contaminates all the downstream region. One should avoid adopting this difference scheme to simulate convection transport if the skew angle falls within this negative numerical diffusion region. The monotonic schemes (1UD/1ED and FA/SKED2), armed with sufficient numerical diffusion, damp out all possible oscillation. The 1UD/1ED scheme significantly smears out the solution profile, especially for large skew angles ($\theta = 30°$ in Fig. 10.2 and $\theta = 45°$ in Fig. 10.3). This phenomenon, which incurs the main criticism on first-order upwind schemes, can be interpreted by the numerical diffusion depicted in Fig. 5.

We may conclude that the suitable monotonic scheme to solve multidimensional convective transport problems is the FA/SKED2 scheme. However, the all positive influence coefficients requirement as fulfilled by the FA/SKED2 scheme is only a sufficient condition to ensure solution monotonicity. In some circumstances, a scheme with negative influence coefficients may still be capable of predicting a monotonic solution, while a scheme with all

positive influence coefficients may induce unnecessary numerical diffusion, smearing out the solution profile around sharp gradients. That is, the numerical diffusion should be controlled and added only when needed.

Based on this reasoning, we may combine two schemes to provide a more accurate and stable approximation of convective transport: one scheme should be an accurate but possible oscillatory scheme and the other should be a stable diffusive scheme. From the discussion above, the obvious choice from the two-dimensional difference schemes for this purpose is the combination of SKED1, which is an accurate scheme free of numerical diffusion, and SKED2, which is a monotonic scheme with minimum numerical diffusion. A simple but effective blending method can be obtained based on these ideas,

$$\phi = \omega\phi_1 + (1 - \omega)\phi_2, \tag{71}$$

where ϕ_1 and ϕ_2 are obtained from SKED1 and SKED2, respectively. The blending factor ω is determined as the maximum value to prevent the occurrence of local extrema,

$$\phi_{\min} \le \phi \le \phi_{\max}, \tag{72}$$

where $\phi_{\min}$ and $\phi_{\max}$ are the minimum and maximum values of a dependent variable at neighboring points. The possible value for ω is in [0, 1]. This strategy is quite close to the filtering technique such as the flux-corrected transport (FCT) proposed by Boris and Book [35, 36]. The blending factor can be explicitly determined in terms of the cell Reynolds number and values of a dependent variable at neighboring computational points. However, in practical computations, we employ an easier procedure to ensure solution monotonicity. Solution of the high-order scheme ϕ_1 is calculated and checked to satisfy the solution boundedness criterion in Eq. (72). If $\phi_{\min} \le \phi_1 \le \phi_{\max}$, then $\phi = \phi_1$ ($\omega = 1$). But if $\phi_1 < \phi_{\min}$ then $\phi = \phi_{\min}$ and if $\phi_1 > \phi_{\max}$ then $\phi = \phi_{\max}$. This simpler procedure is equivalent to choosing a maximum blending factor satisfying Eq. (72) and the resulting numerical diffusivity is

$$\Gamma_N = (1 - \omega)\Gamma_{N,\mathrm{SKED2}}, \tag{73}$$

where $\Gamma_{N,\mathrm{SKED2}}$ is the numerical diffusivity for SKED2, which can be found in Table I. Thus, it is not necessary to explicitly determine the value of blending factor in the present calculations to find the resulting solution. However, its value and the corresponding numerical diffusivity can be obtained if the resulting solution ϕ, ϕ_1, and ϕ_2 are known. Similar treatment can be found in Sharif and Busnaina [22], who adopted the SKUD scheme as the accurate scheme to provide the bounded solutions. Therefore, the numerical diffusion is added sparingly with the minimum amount to avoid an unbounded solution inflicted by the accurate difference scheme ϕ_1.

Figure 10.4 illustrates the solution resulting from blending as compared with those obtained from the original schemes SKED1 and SKED2. The prediction accuracy is significantly increased with this simple blending technique. Therefore, selection of SKED1 and SKED2 to obtain the blended solution in the present study is quite reasonable.

5.2.2. Convective Transport with Physical Diffusivity. The second problem considered is similar to the above problem but with physical diffusivity. The cell Reynolds number will be finite and, in the present calculations, its value is taken as 50,

$$R_h = \frac{|V|h}{\mu} = 50. \tag{74}$$

The approximate solution can be found with a similarity transformation by neglecting the streamwise diffusion [19]. Figures 11.1–11.3 depict the computational results at various flow skew angles of $\theta = 15°$, $\theta = 30°$, and $\theta = 45°$. These results can be compared with those given in Figs. 10.1–10.3 for the previous problem without physical diffusivity. As one can expect, the existence of physical diffusion will alleviate the steep change in the solution profile and all the difference schemes yield more accurate results. The existing overshoots and undershoots predicted by oscillatory schemes are also decreased. Especially for the SKUD scheme at $\theta = 30°$ shown in Fig. 11.2, the persistent wiggle distribution in the downstream region disappeared, owing to the damping effect introduced from the physical diffusivity. This can be found from the numerical diffusion shown in Fig. 5.2. However, similar trends can be observed between Figs. 11.1–11.3 and Figs. 10.1–10.3, since this problem is also a convection-dominated one. Identical schemes in the limiting pure convection transport (1UD and 1ED, 2UD, and 2ED, and FA and SKED2) are no longer the same, due to the existence of physical diffusion.

Slight variations between these schemes can be found. The exponential difference schemes (1ED and 2ED), with the convection and diffusion effects simultaneously considered, can, in general, yield a more accurate prediction than the upwind difference schemes (1UD and 2UD). As for FA and SKED2, they will provide an almost identical solution if the skew angle is not too large ($\theta = 15°$ in Fig. 11.1, and $\theta = 30°$ in Fig. 11.2). However, if the velocity direction nearly aligns with the grid diagonal line ($\theta = 45°$ in Fig. 11.3), the FA method will yield a solution with more numerical diffusion than the SKED2 scheme. One can refer this phenomenon to the numerical diffusivity shown in Fig. 5.3 for FA and Fig. 5.5 for SKED2. Therefore, in terms of computational efficiency and prediction accuracy, the SKED2 scheme is proven to be superior to the FA method.

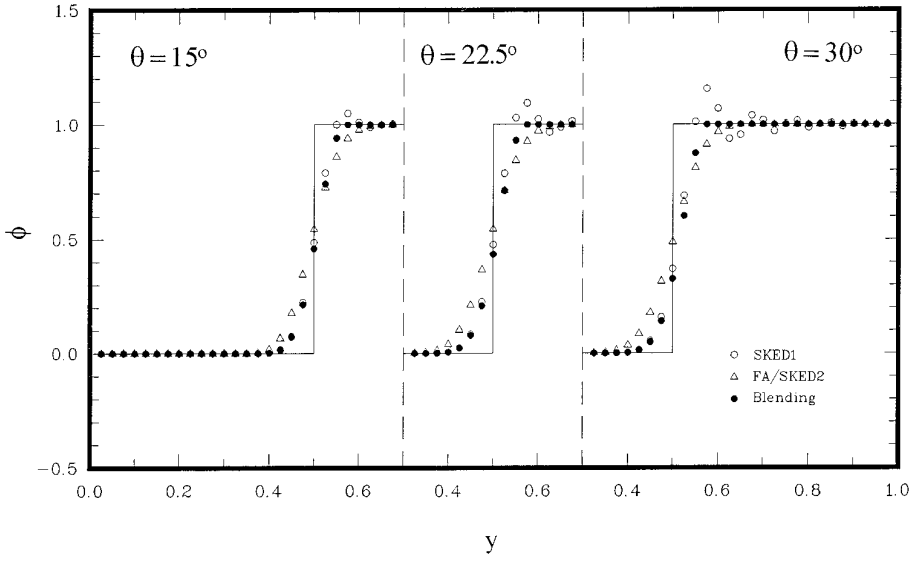

FIG. 10.4. Computational results with the blending procedure.

The blending procedure given in Eq. (71) is also used to solve this problem and the results are depicted in Fig. 11.4. As compared with pure convection situation shown in Fig. 10.4, it is clear that this blending procedure is still very effective to raise the computational accuracy.

5.2.3. The Diffusion Dominant Problem. The last problem to verify the performance of difference schemes is a diffusion dominant problem with a small cell Reynolds number,

$$R_{x,h} = \tfrac{1}{4}\cot(\theta), \quad R_{y,h} = \tfrac{1}{4}. \tag{75}$$

The boundary conditions are

$$\Phi(x,0) = \Phi(x,1) = \Phi(1,y) = 0 \tag{76}$$

and

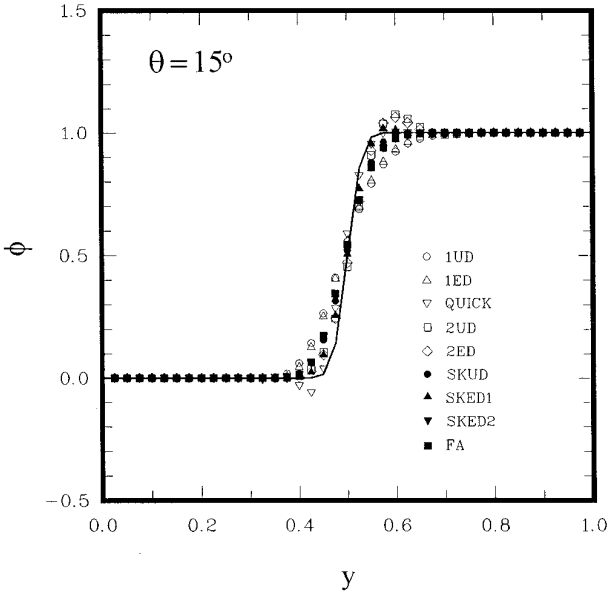

FIG. 11.1. Computational results at $\theta = 15°$.

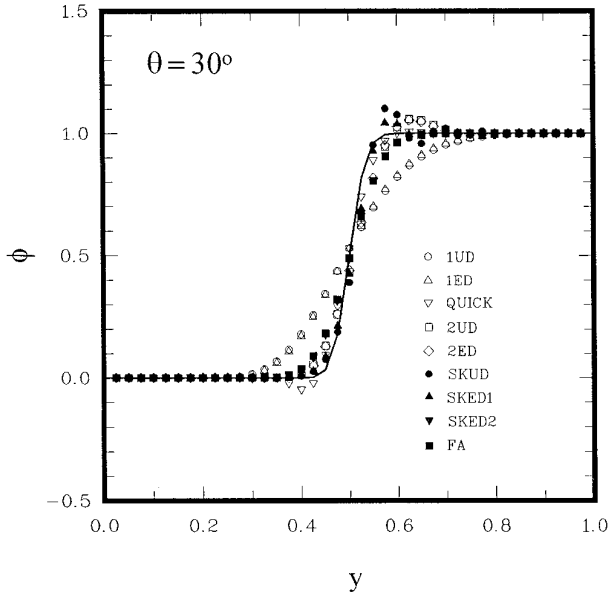

FIG. 11.2. Computational results at $\theta = 30°$.

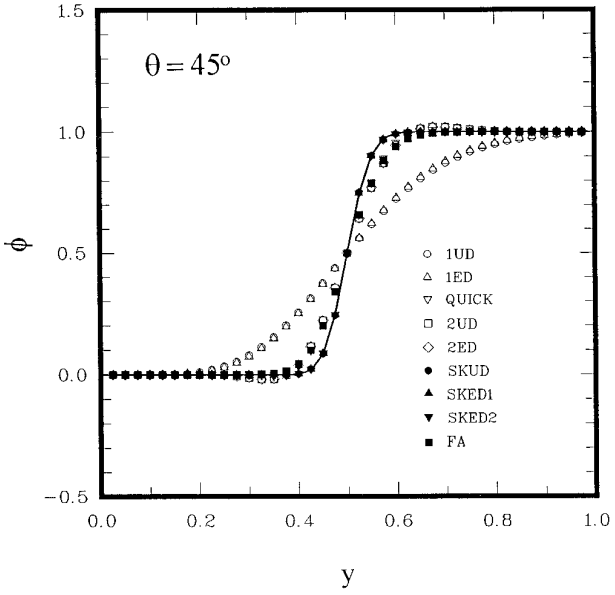

FIG. 11.3. Computational results at $\theta = 45°$.

$$\Phi(0, y) = \Phi_0 \exp\left[\frac{v}{2}(y - y_s)\right] \sin(\pi y),$$

where

$$\Phi_0 = \frac{1}{\sin(\pi y_s)}, \quad y_s = 1. - \frac{1}{\pi}\tan^{-1}\left(\frac{2\pi}{v}\right).$$

The exact solution can be found by the separation of variables,

$$\Phi(x, y) = \frac{\Phi_0}{1 - \exp(r_2 - r_1)} \sin(\pi y) \exp(r_2 x) \{1. - \exp[(r_1 - r_2)(x - 1)]\}, \tag{77}$$

where

$$r_1 = \tfrac{1}{2}[u + \sqrt{u^2 + v^2 + 4\pi^2}], \quad r_2 = \tfrac{1}{2}[u - \sqrt{u^2 + v^2 + 4\pi^2}].$$

This problem was proposed by Bradley *et al.* [37] to test their third-order scheme for convection problems based on Taylor-series expansion. Computational results along with exact solution at $x = 0.5$ by various difference schemes for the skew angles $\theta = 15°$, $\theta = 30°$, and $\theta = 45°$ are shown in Figs. 12.1–12.3, respectively. As illustrated in these figures, all the exponential-related difference schemes (1ED, 2ED, SKED1, SKED2, and FA), which simultaneously consider the convection–diffusion effects, as well as the QUICK scheme, yield very accurate solutions. The QUICK scheme presents a highly accurate treatment for the convection term. On the other hand, all the upwind schemes (1UD, 2UD, and SKUD) obviously provide the computational results with too much numerical diffusion. It is also quite interesting that the SKUD scheme, with even less cross-stream numerical diffusion, yields a less accurate solution than the simple 1UD scheme. This phenomenon implies that the streamwise numerical diffusion cannot be ignored if the diffusion transport is comparable with the convection. Meanwhile, the exponential schemes seem to be the suitable candidates to alleviate this streamwise numerical diffusion.

6. CONCLUSIONS

From the viewpoint of the finite volume formulation, convective transport is difficult to simulate because the mass flux flowing out of the control volume will produce a negative effect on the accumulation of the transported quantity within the control volume. This is the physical reason why the upstream difference schemes can yield stable discretizations. However, the simple upwind scheme (first-order) cannot provide a sufficiently accurate solution in practical computations with reasonable grid spacing. On the other hand, higher-order schemes will inevitably induce oscillatory results if there exist some strong solution gradients. Mathematically, this problem with an unbounded solution can be attributed to the numerical dispersive error of a finite difference scheme with insufficient diffusion to damp out the undesirable oscillations. Exponential difference schemes, which originate from the simultaneous consideration of convection and diffusion effects, are reasonable candidates to overcome this problem because the exact distribution of the convection–diffusion equation involves some kinds of exponential functions.

In the one-dimensional equation without a source term, the simple exponential difference scheme can provide the exact solution without any oscillation. However, criticism on this scheme still remains: its accuracy will decline in cases of the existence of a nonconstant source term or in multidimensional problems. The present work is then devoted to resolving these problems. First, we derive a second-order exponential difference scheme based on one-dimensional analysis. Exponential functions are introduced to depict the relative importance of influence coefficients for neighboring points in the resulting difference equation. Asymptotic properties of this proposed scheme are analyzed in the limits of diffusion- and convection-dominant situations. For diffusion-dominant situations, the second-order exponential difference scheme will become fourth-order accurate from the Taylor-series truncation error analysis; while for the convective-dominant situation, it will be identical with the existing second-order upwind difference scheme. The characteristic roots of the difference equation are all positive for any combination of diffu-

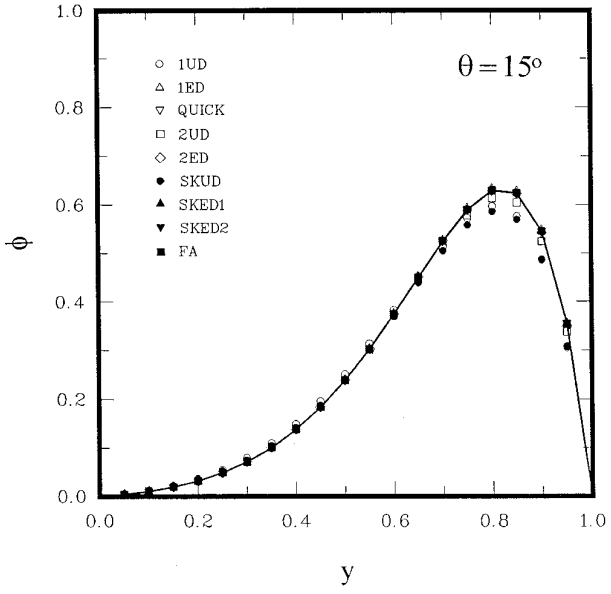

FIG. 12.1. Computational results at $\theta = 15°$.

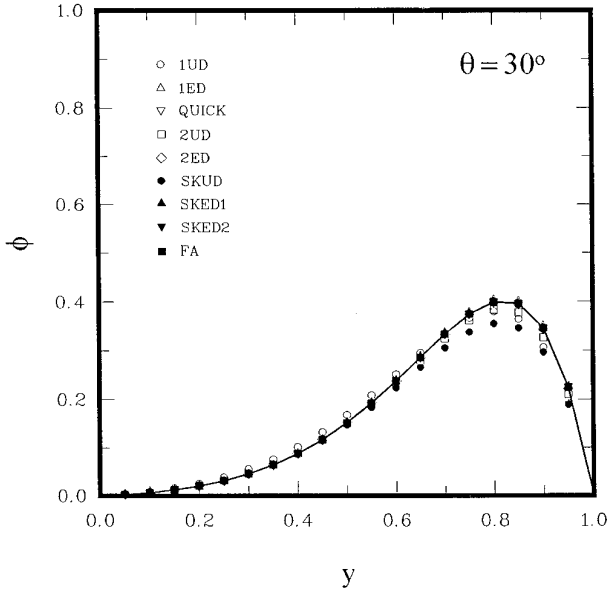

FIG. 12.2. Computational results at $\theta = 30°$.

sion and convection transports, which implies that the persistent oscillation problem in the solution will not occur. From the numerical experiments, this is a plausible scheme to provide the difference representation of convection–diffusion equation. Meanwhile, the order accuracy of this scheme will not decrease when there are source terms or in multidimensional problems.

The second achievement in the present work is to provide a simple but effective local particular solution method in recovering the accuracy of the first-order exponential difference scheme with a nonconstant source term. We analyze methematically the deterioration in accuracy of the exponential difference scheme due to the introduction of a source term and the effectiveness of the local particular solution method. In this method, the equation is locally transformed to a source-free problem where an accurate solution can be obtained with the first-order exponential difference scheme. A general expression for any source term based on a polynomial fitting procedure is also proposed to obtain the local particular solution. Performance

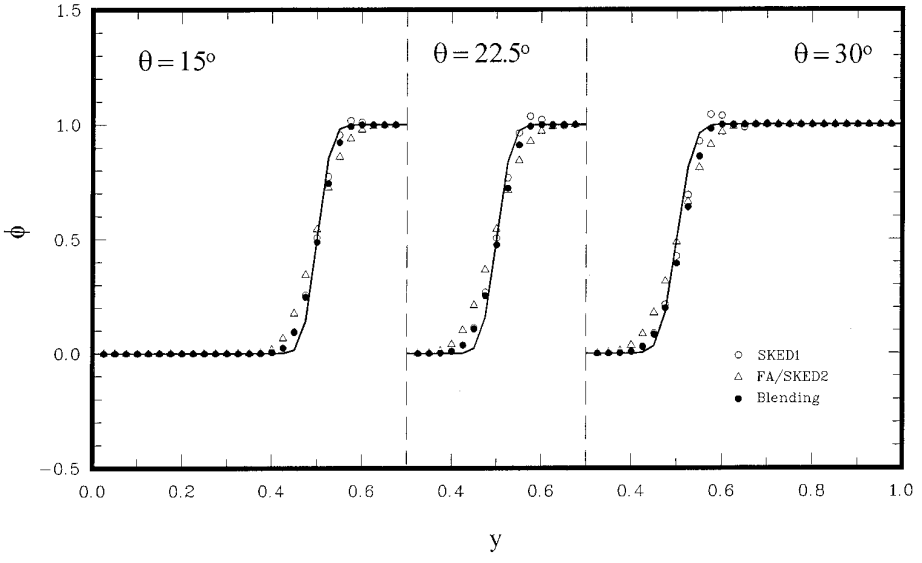

FIG. 11.4. Computational results by the blending procedure.

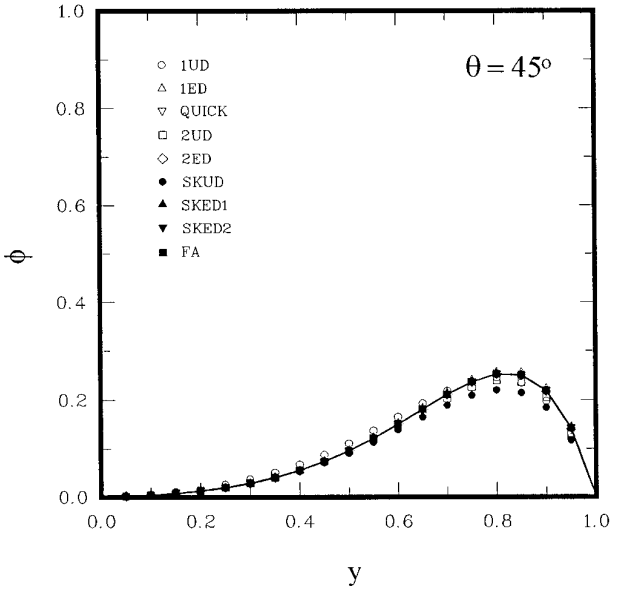

FIG. 12.3. Computational results at $\theta = 45°$.

of this proposed technique is verified by solving several test problems and the results show that it is quite effective to increase the prediction accuracy.

For two-dimensional problems, we derive a cross-stream numerical diffusivity to signify the accuracy of the skew difference schemes that incorporate the influences of corner points in the discretizations. Based on the Taylor-series truncation error analysis, all the skew difference schemes are only first-order accurate in one-dimensional situations. However, their accuracy for multidimensional problems can be maintained in convection dominated flows if the cross-stream numerical diffusion can be effectively eliminated. In the present work, we propose two skew exponential difference schemes to model the two-dimensional convection–diffusion equation. One is derived to be free of numerical diffusion and should be an accurate representation for problems with a moderate solution gradient. The other is devised to have minimal numerical diffusion to ensure monotonic solutions if there exist some steep changes in the solution. Some existing skew difference schemes are also analyzed to find their corresponding numerical diffusion. The results show that our proposed schemes will be superior to these skew difference schemes in terms of the prediction accuracy and programming simplicity. Numerical calculations of some test problems also verify that the cross-stream numerical diffusion derived in the present study is a feasible error indicator for skew-difference schemes.

Finally, we suggest a simple blending procedure of the two exponential difference schemes proposed herein to achieve a more accurate and stable discretization for all possible flow situations, with or without solution discontinuities. This blending technique is based on the reasoning that the numerical diffusion should be added only when it is truly needed and by the minimum amount to prevent solution oscillation. Numerical calculations reveal that this simple modification is quite effective to obtain accurate and stable solutions in several test problems. Therefore, we can conclude from the present analyses and numerical experiments that the exponential difference schemes can be employed to accurately solve the convection–diffusion problems. Criticism of their accuracy in the existence of source term and in multidimensional problems can be alleviated. These exponential difference schemes deserve further investigations in more complicated situations.

The present study is confined in the steady flow calculations. As for unsteady flow situations, two simple strategies can be suggested to treat the transient term by incorporating the analyses presented here. One is treating the transient term as a source term and employing the local particular solution method to derive its appropriate discretized expression. The other method is taking the time derivative term as a pseudo-spatial dimension without physical diffusivity. Techniques developed in the present work can be used to find the corresponding exponential difference approximation but with an additional dimension. This procedure, as one may expect, will involve more complicated derivations and resulting computations.

REFERENCES

1. O. R. Burgraff, *J. Fluid Mech.* **24,** 113 (1966).
2. E. F. F. Botta and A. E. P. Veldman, *J. Comput. Phys.* **48,** 127 (1981).
3. J. D. Bozeman and C. Dalton, *J. Comput. Phys.* **12,** 348 (1973).
4. D. B. Spalding, *Int. J. Numer. Methods Eng.* **4,** 551 (1972).
5. M. K. Patel, N. C. Markatos, and M. Cross, *Int. J. Numer. Methods Fluids* **5,** 225 (1985).
6. P. J. Roache, *ASME J. Fluids Eng.* **116,** 405 (1994).
7. B. P. Leonard, *Comput. Methods Appl. Mech. Eng.* **19,** 59 (1979).
8. M. Atias, M. Wolfshtein, and M. Israeli, *AIAA J.* **15,** 263 (1977).
9. M. M. Gupta and R. P. Manohar, *AIAA J.* **16,** 759 (1978).
10. W. Shyy, *J. Comput. Phys.* **57,** 415 (1985).
11. S. G. Rubin and P. K. Khosla, *J. Comput. Phys.* **24,** 217 (1977).
12. T. Saitoh, *Int. J. Numer. Methods Eng.* **11,** 1439 (1977).
13. R. K. Agarwal, AIAA-81-0112, 1981 (unpublished).
14. Z. Lilek and M. Peric, *Comput. & Fluids* **24,** 239 (1995).
15. M. A. Leschziner, *Comput. Methods Appl. Mech. Eng.* **23,** 293 (1980).
16. T. Han, J. A. C. Humphrey, and B. E. Launder, *Comput. Methods Appl. Mech. Eng.* **29,** 81 (1981).
17. A. Pollard and A. L.-W. Siu, *Comput. Methods Appl. Mech. Eng.* **35,** 293 (1982).
18. W. Shyy, *Computational Modeling for Fluid Flow and Interfacial Transport* (Elsevier, Amsterdam, 1994), p. 103.
19. G. D. Raithby, *Comput. Methods Appl. Mech. Eng.* **9,** 153 (1976).
20. M. A. Leschziner and W. Rodi, *ASME J. Fluids Eng.* **103,** 352 (1981).
21. P. G. Huang, B. E. Launder, and M. A. Leschziner, *Comput. Methods Appl. Mech. Eng.* **48,** 1 (1985).

22. M. A. R. Sharif and A. A. Busnaina, *J. Comput. Phys.* **74,** 143 (1988).
23. G. D. Raithby and K. E. Torrance, *Comput. & Fluids* **2,** 191 (1974).
24. G. D. Raithby, *Comput. Methods Appl. Mech. Eng.* **9,** 75 (1976).
25. J. C. Chien, *Comput. & Fluids* **5,** 15 (1977).
26. B. P. Leonard and J. E. Drummond, *Int. J. Numer. Methods Fluids* **20,** 421 (1995).
27. G. D. Stubley, G. D. Raithby, A. B. Strong, and K. A. Woolner, *Comput. Methods Appl. Mech. Eng.* **35,** 153 (1982).
28. C.-J. Chen and H.-C. Chen, *J. Comput. Phys.* **53,** 209 (1984).
29. S. V. Patankar, *Numerical Heat Transfer and Fluid Flow* (Hemisphere, New York, 1980), p. 90.
30. M. R. Spiegel, *Mathematical Handbook* (McGraw–Hill, New York, 1968), p. 32.
31. F. B. Hildebrand, *Advanced Calculus for Applications* (Prentice–Hall, Englewood Cliffs, NJ, 1976), Chap. 8.
32. G. De Vahl Davis and G. D. Mallinson, *Comput. & Fluids* **4,** 29 (1976).
33. M. Wolfshtein, Imperial College Mechanical Engineering Department Report SF/R/2, 1967 (unpublished).
34. H. S. Carslaw and J. C. Jaeger, *Conduction of Heat in Solids* (Oxford Univ. Press, London, 1959), p. 41.
35. J. P. Boris and D. L. Book, *J. Comput. Phys.* **11,** 38 (1973).
36. D. L. Book, J. P. Boris, and K. Hain, *J. Comput. Phys.* **18,** 248 (1973).
37. D. Bradley, M. Missaghi, and S. B. Chin, *Comput. Methods Appl. Mech. Eng.* **69,** 133 (1988).